Sodium amidoborane - a dead end for solid-state hydrogen storage or a gateway to advanced energy systems?

Igor Milanović[†] and Nikola Biliškov[*,‡]

[†] *Vinča Institute of Nuclear Sciences, National Institute of the Republic of Serbia, Centre of Excellence for Renewable and Hydrogen Energy, The University of Belgrade, POB 522, 11000 Belgrade, Republic of Serbia*

[‡] *Rudjer Bošković Institute, Bijenička c. 54, 10000 Zagreb, Croatia*

E-mail: nbilis@irb.hr

Phone: +385 1 4561084

Abstract

Alkali metal amidoboranes have been intensively investigated as potentially highly attractive candidates for solid-state hydrogen storage. In this family, sodium amidoborane $NaNH_2BH_3$ occupies a special place, due to its unique properties. From one side, its high hydrogen content (9.4 wt.%) and low dehydrogenation temperature (89 °C) make it very perspective in this regard. However, detailed studies revealed a number of very serious drawbacks, which consequently led to a dramatic reduction of the initial research hype, although potentially very interesting innovative aspects of its use beyond hydrogen storage have also been discovered. However, a critical insight to the entire field of metal amidoborane chemistry, especially in the technologically relevant context of solid-state hydrogen storage, is lacking. Thus, by this review, we want to fill this gap. Accordingly, this review brings a detailed and critical comparative discussion

of synthesis and chemical properties of sodium amidoborane. They are considered not exclusive through technological, but also environmentally relevant optics with respect of their utilization in real-world advanced and sustainable energy systems.

Introduction

A broader context - climate crisis and energy transformation

Currently dominating socio-economic system translated into a way of living is mainly driven by combustion of carbon-rich fossil fuels. This directly results in harmful emissions of enormous amounts of CO_2. According to the best available science, these anthropogenic CO_2 emissions are the main cause of current climate changes, undoubtedly evidenced in the past and current century.[1–4] Today, the human population exceeded 8 billion, and it is estimated to exceed 9 billion by 2050.[5,6] According to International Energy Agency (IEA), the global energy demand will rise by nearly 50 % by 2050.[7] Currently dominant fossil fuel-powered energy systems have supported the industrial revolution together with most of its benefits leading to population growth, including the extension of our life expectancy, economic development, and associated societal order. However, they also cause geopolitical tensions, growing inequality, as well as economic growth of one part of the world at the expense of underdeveloped societies of the so-called Global South.[8] The critical imperative of phasing-out fossil fuel-based energetics and its rapid transformation to renewable sources, imposed by climate crisis, makes meeting these requirements technologically enormously challenging.[9]

Energy transition must be just. In the other words, renewable sources must satisfy the energetic needs of the civilization in order to sustain the current standard of living, but it must not be carried out to the detriment of underdeveloped parts of the world. It must be implemented globally, seriously taking into account the principles of climate justice, in order to meet both temporal and spatial societal and environmental sustainability.[3]

In practice, this means that renewable sources must become economically and energeti-

cally not only concurrent but more admissible to currently dominant fossil fuels. Narratively, they must cease to be alternatives and become major and, in short term, exclusive sources of energy. The climate goals are clearly set by Paris agreement to limit global warming to well below +2 °C, preferably not more than +1.5 °C, compared to pre-industrial levels,[10] and they are translated to directives at international levels[11] and to national political goals and legislation to prevent catastrophic and irreversible climate change. This goal is not unreachable - more than 100 years ago, "the father of photochemistry" Giacomo Ciamician clearly argued that our civilisation is technologically ready to switch from fossil fuels to renewable sources of energy.[12] From the energetic point of view, to reach this ambitious, but indispensable goal, the problems caused by inherent intermittent energy delivery[13] from renewable sources must be overcame by implementation of efficient systems for energy storage. Various technological concepts of energy storage are currently available or under development,[14] and they can be simply divided to mechanical and chemical. Among chemical concepts, the most important representatives are various batteries, supercapacitors and hydrogen storage.

This review is focused on one very specific family of candidate systems for solid-state hydrogen storage. In order to address the title question, in very broad context of climate change it is reformulated to more specific questions, and the most important are: 1. Is the use of the material limited to hydrogen storage or they are applicable in some other energy-related technologies? 2. How successful is the material when compared to other options? 3. Are the all steps of production and use of this material environmentally sustainable?

A deeper context - the concept of solid-state hydrogen storage

As the lightest element, hydrogen has a large gravimetric energy density of $120\,\mathrm{MJ\,kg^{-1}}$, which is approximately three times higher than that of gasoline. However, due to the low density in both gas and liquid state, the volumetric energy density is extremely low ($5.6\,\mathrm{MJ\,dm^{-3}}$ at 70 MPa). Therefore, conventional storage of hydrogen in gas or liquid phase provides only a limited energy content. Density of solid hydrogen, which exist only at extremely low tem-

peratures, is only slightly higher than liquid H_2 (0.076 for solid and 0.071 g/cm^3 for liquid H_2, respectively). Thus, it is not considered for any real-world practical use. However, solid-state chemisorptive storage provides the highest number density of hydrogen.[15] As a guideline for development of hydrogen storage systems for mobile use, performance targets were defined by U.S. Department of Energy (US-DOE).[16]

Any successful material for solid-state hydrogen storage must satisfy the following criteria: high (both mass and volumetric) hydrogen capacity, fast hydrogen desorption and absorption kinetics, easy activation, minimal deterioration during cycling, safety and low price. The difficulties associated with development of such systems for hydrogen storage make them a crucial contemporary scientific and technological challenge for the realisation of widespread use of hydrogen as energy carrier in a zero-emission, carbon-free hydrogen economy. It is somewhat rarely mentioned that production of materials should also satisfy the principles of green chemistry,[18–20] which are today increasingly engaged in addressing energy needs through the development of sustainable technologies by sustainable procedures. Although the problem of materials for solid-state hydrogen storage is mainly chemical in its nature, the invention of the effective systems giving hydrogen by solid-state thermal decomposition, which meet all technological and environmental needs, requires an interdisciplinary approach. For sure, this will make far-reaching impact on the industry, and indirectly to society as a whole.

Materials for solid-state hydrogen storage

In order to address the central question of the title of this review, it is crucial to evaluate ammonia borane and amidoboranes as potential materials for hydrogen storage, as well as their applicability in other energy-related concepts. In this regard, the research interest in these materials is shortly considered here. Fig. 1 and scientometric analysis[21] show that the research in the field of hydrogen storage goes through a hype-disappointment cycles, largely driven not exclusively by scientific curiosity, but also by political will to support hydrogen-

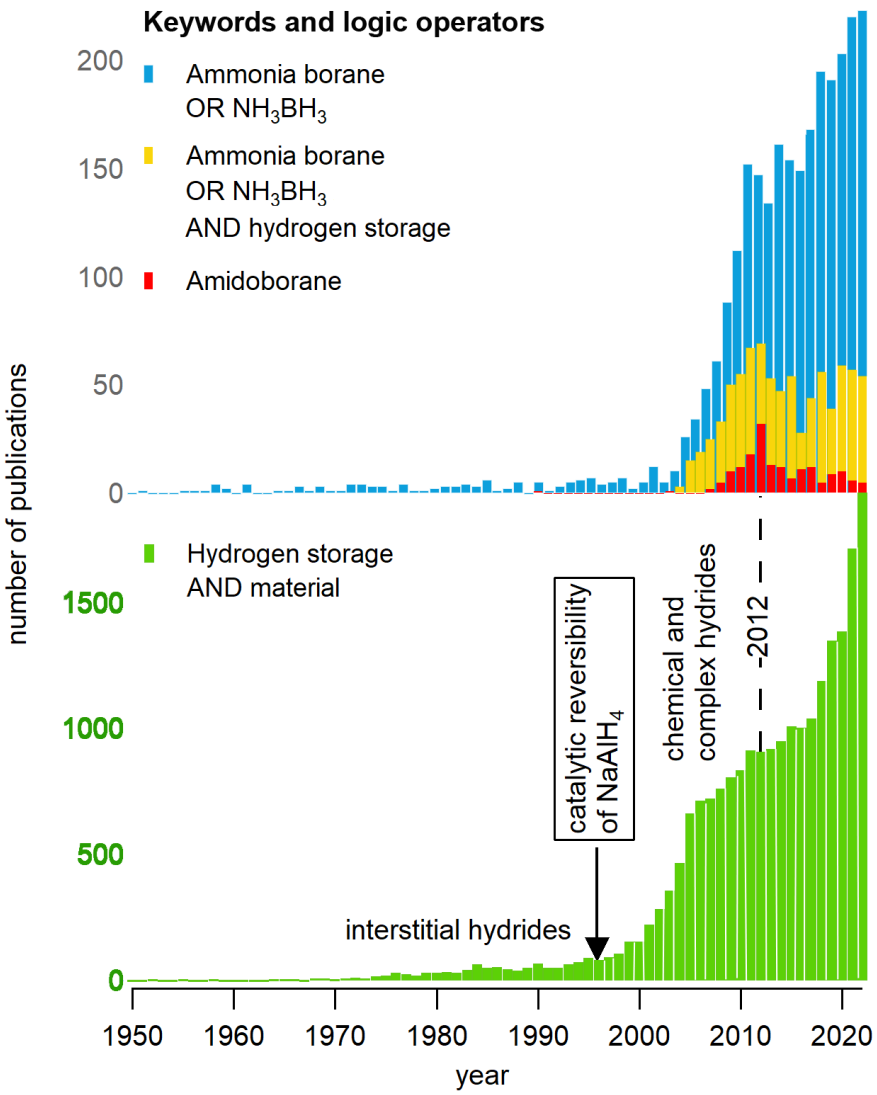

Figure 1: Number of publications related to solid-state hydrogen storage, ammonia borane and amidoboranes over time. Inserted text denotes the dominant focuses of materials science related to hydrogen storage. Bogdanović's publication on TiO_2 doping-induced reversibility of $NaAlH_4$ dehydrogenation[17] led to a change in research focus from intermetallics to chemical and complex hydrides. This coincides with appearance of HAB on the scene, which is followed by re-discovery of amidoboranes, which, however, lasted over just a short period. Note that the publications focused to dehydrogenation methods other than those in solid state were not considered here. Source: Scopus (accessed Feb. 17, 2023)

related research. At first, there were overly optimistic expectations for the development of technologies. This, for example, coincides with seminal publication by Bogdanović on doping of $NaAlH_4$ with $TiCl_3$, which led to reversible dehydrogenation of the material,[17] thus opening the door for the intense research on chemical[22] and complex hydrides.[23,24] However, it is followed by a "disappointment phase", which began at the end of the first decade of this century, reflected by a plateau in the 2012-2015 period, as the development revealed to be slower than the inflated expectations.

After this stagnation, the novel, still ongoing interest in hydrogen storage is evident (Fig. 1), which coincides with significantly increased political support to hydrogen-related research. The new classes of materials, such as metal-organic frameworks (MOF) and borohydrides came to the scene after 2004, taking the dominant position, while the interest for $LaNi_5$-type alloys and carbon nanotubes is stagnant and declining. Metal hydrides (e.g. MgH_2) are present through the entire period with growing number of publications. Regarding ammonia borane and amidoboranes, Fig. 1 shows an exponential increase of the number of publications evident over the first decade of this century. However, the year 2012 marks a turning point in this field: while the number of publications on ammonia borane continues to grow, although turning from exponential to linear trend, a significant decrease of the number of amidoborane-related publications is evident. It is important to note that, after this point, the growing number of publications on HAB is mainly associated with its applications for purposes other than hydrogen storage (Fig. 1). This indicates a serious disappointment of the researchers by this class of materials. The number of publications on amidoboranes is dramatically decreased after the initial research hype. Simultaneously, HAB is evidently still considered for hydrogen storage, at least by some groups, but this interest is stagnating or even slowly dropping for more than a decade. However, the evident loss of research interest still does not necessary means that these materials are really useless for hydrogen storage or any other application. Thus, one of the purposes of this review is to check the justification and foundation of described trends. Obviously, a number of excellent reviews cover various

aspects, especially those relevant to hydrogen storage-related utilization of HAB[25–28] and metal amidoboranes (MAB).[29–33] However, they are mainly focused to structural properties, synthetic methods and dehydrogenation, with little or no critical discourse to their actual utility and benefits that their wider use would bring. On the basis of our research findings and experience in the field of chemistry of HAB and metal amidoboranes, the main conclusion is that they are generally characterized by an extremely complex chemistry, which is very sensitive to large number of physical and chemical perturbations from the environment, making their behaviour pretty much hard to control. The overall high reactivity of NaH + HAB system and derived NaAB makes it an especially interesting system, but not so much in the field of hydrogen storage. We will try to show that its potential applications arise precisely from the high reactivity and microscopic dynamics of this system. Thus, it is important to critically reconsider the entire family and chemistry of their members. By this review, on the firm basis of physico-chemical properties of these systems, we will try to bring the discussion of these aspects to the fore, thus proposing some ideas and guidelines for further research in this field.

The results of this work and the recent launch of commercial hydrogen cars, trains and stationary solutions for hydrogen production and fuel cells, indicate that, although the hydrogen energy field as a whole is transitioning from small-scale (lab and prototype stage) to large-scale (commercial deployment), materials-based hydrogen storage is still requiring technological challenges to be overcome. Therefore more scientific research is needed before extensive commercial deployment can be realized.

During the last two decades much efforts have been made in searching for adequate hydrogen storage material which would be reversible, which possesses high gravimetric and volumetric hydrogen capacity, fast dehydrogenation kinetics and low dehydrogenation temperature. Still, there is no "perfect" material for solid-state hydrogen storage. Various classes of materials are investigated in this regard, and they are summarized in Fig. 2. The investigated materials for hydrogen storage are mainly different hydrides: interstitial

hydrides of intermetallic phases (e.g. $LaNi_5$-type intermetallics),[34,35] metal hydrides (e.g. MgH_2),[36–40] complex hydrides (e.g. $NaBH_4$,[41–44] $NaAlH_4$[17,23,45–49]) and chemical hydrides such as boron-nitrogen-hydrogen containing compounds (e.g. NH_3BH_3),[50–52] which are all presented in Fig. 2. Additionally, a very interesting in this regard are porous systems, which can confine hydrogen in its structure by physisorption. The representative members of this group include metal organic frameworks (e.g. Zn_4O(1,4-benzenedicarboxylate)),[53] carbon nanotubes,[54] carbon cryogels,[55,56] and other nanoscaffold structures.[57]

It is evident that physisorptive materials exhibit high gravimetric capacities and are on-board reversible with facile kinetics. However, the major drawback is contained in their poor volumetric capacity and very low hydrogen sorption energies, which require cryogenic temperatures for their practical use. Interstitial hydrides of intermetallic phases are characterized by a very high volumetric capacities, favorable kinetics, efficiencies and thermodynamics, and they are on-board reversible. However, their very nature carries unsurmountable disadvantages: they are typically made of lanthanide-based intermetallics, making them very expensive, and causing very low gravimetric capacities. Additionally, the abundance of lanthanides is very limited, and the ore processing to obtain pure metals is energetically very demanding. High gravimetric and volumetric capacities are typical for complex hydrides, where amidoboranes belong. At least some of them are also potentially on-board reversible, because favorable thermodynamics is characteristic for a number of these materials. However, their H_2 uptake/release kinetics is poor and unfavourable. Finally, chemical hydrides (ammonia borane is a typical member of this family) possess high volumetric and gravimetric H_2 capacity, but their typically highly exothermic dehydrogenation makes them practically irreversible and energy inefficient.[58]

Characterization methods

In the context of this review, the purpose of the most commom methods for characterization is to identify and understand the physics and chemistry underlying fundamental properties

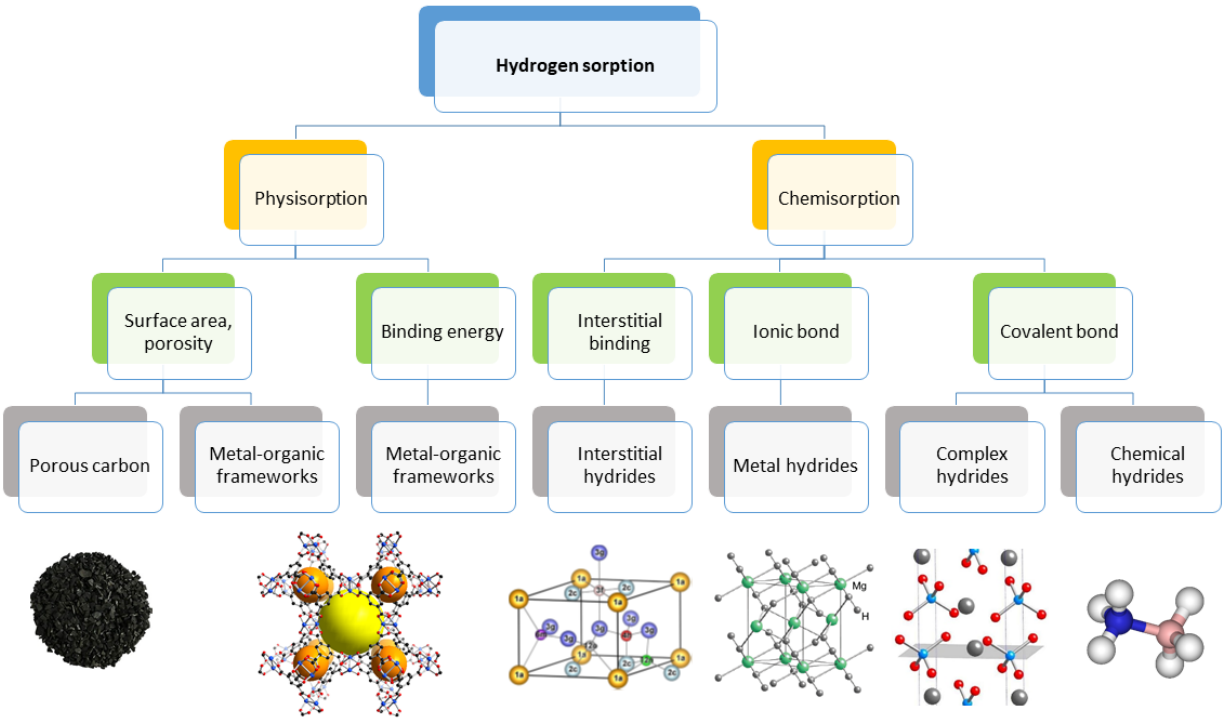

	Interstitial hydrides	Metal hydrides	Porous materials	Complex hydrides	Chemical hydrides
	$LaNi_5H_6$ and other hydrides of intermetallic compounds	MgH_2, NaH, LiH,...	Metal-organic frameworks, covalent organic frameworks, zeolites, porous carbon,...	Alanates, borohydrides, amides, amidoboranes,...	NH_3BH_3
Volumetric capacity					
Gravimetric capacity					
Thermodynamics					
Desorption thermodynamics	Endothermic	Endothermic	Slightly endothermic	Mainly endothermic	Exothermic
Kinetics					
Reversibility					
Efficiency					
Abundance					

Figure 2: Overview of the main classes of materials for solid-state hydrogen storage and their relevant properties. Their advantages and disadvantages with respect to DOE targets[16] are delineated by colored fields: red indicates significant challenges, green signifies satisfactory performance, and yellow indicates that some improvement is required. Reversibility and performance in real-world conditions are indicated in terms of and thermodynamics.

relevant to the utilization of a material for hydrogen storage at laboratory scale. These properties include molecular and crystal structure of the material, hydrogen capacity, kinetics and thermodynamics of relevant processes, such as absorption and desorption of hydrogen, and cycle-life.

To elucidate the structure, commonly used technique is single-crystal or powder X-ray diffraction (SCXRD and PXRD). SCXRD gives highly accurate structure of molecules and their arrangement in crystal. It is restricted to single crystals. In most practical cases, samples are available only in multicrystalline powdered form, and in this case the researcher is limited to PXRD, which in principle contains structure information, but the molecular structure cannot be determined at highest possible accuracy, as in the case of SCXRD. However, PXRD is very sensitive to phase composition of the sample, so it is commonly used to determine the relative amount of crystalline phases present in the material. Nowadays, it is also commonly employed to monitor the mechanochemical syntheses of various crystalline materials, including materials for solid-state hydrogen storage,[59] as well as evolution of the system during the dehydrogenation. Molecular spectroscopies, among which most commonly used infrared (IR) and Raman spectroscopy, give a direct insight into vibrational properties of the material, and thus to its intra- and intermolecular structure and organization. The methods are highly sensitive to microscopic molecular environment. In practice, this means that a change in environmental conditions affect the vibrations of particular functional groups. In IR and Raman spectra, this change in vibration will be observed as change of some or all parameters of the spectral band due to this vibration. The methods are not restricted to crystalline materials, which altogether makes them crucial to fully understand fundamental aspects of materials for solid-state hydrogen storage.[60] Important structural information is also provided by solid-state nuclear magnetic resonance (NMR) spectroscopy. Since this method gives anisotropic part of spin interactions in solid state, the spectra are characterized by broader lines with respect to liquid-state NMR, thus making them applicable for elucidation of quantitative information on molecular structure, conformation and

dynamics. Since ^{11}B, ^{14}N and ^{1}H nuclei are NMR active,[61–64] all of them can be considered in the field of amidoboranes. Additionally, any heteronuclear combination is also possible.[65]

Thermodynamic measurements mostly imply differential scanning calorimetry (DSC)[66] and various forms of thermogravimetry (TG).[67] These methods can be mutually coupled or coupled with spectroscopic and kinetic measurements, in order to give more detailed information on the considered process. It is important to note that thermodynamic properties or thermodynamics of particular processes can be also elucidated by means of other, such as temperature-dependent structural and spectroscopic methods.

A direct information of hydrogen sorption and desorption, such as kinetic and volumetric aspects of this process, is mostly obtained by volumetric or manometric measurements or by applying spectroscopic methods sensitive to the concentration of hydrogen and other present gases. Traditionally, due to their direct implication to technological utilization, pressure-composition isotherms are the most reported and hydrogen storage properties of the materials. They are commonly measured by Sievert method, which can be combined with porosimetry.[68] However, this property is of limited importance in the case of chemical and complex hydrides, since for the utilization of these materials the other properties, siuch as absorption/desorption kinetcs and the purity of released H_2 come to the fore. In this regard, mostly used methods imply temperature programmed desorption (TPD),[69] which is in principle a heating system coupled with a method for analyis of the composition of released gas, most commonly quadrupole mass spectroscopy for evolving gas analysis (EGA-QMS),[70] but it can be also IR spectroscopy.[71,72]

Ammonia borane

Ammonia borane (NH_3BH_3, sometimes named borane-ammonia complex or borazane, further in the text HAB) is the simplest member of the amine-boranes.

It was obtained in 1955[73] by metathesis reaction from $LiBH_4$:

$$LiBH_4 + NH_4Cl \xrightarrow{Et2O} NH_3BH_3 + LiCl + H_2 \tag{1}$$

or

$$2\,LiBH_4 + (NH_4)_2SO_4 \xrightarrow{Et2O} 2\,NH_3BH_3 + Li_2SO_4 + 2\,H_2 \tag{2}$$

Today, HAB is obtained in highest yields by:[74]

$$NH_4Cl + NaBH_4 \xrightarrow{\text{anh. NH3 / THF}} NH_3BH_3 + NaCl + H_2 \tag{3}$$

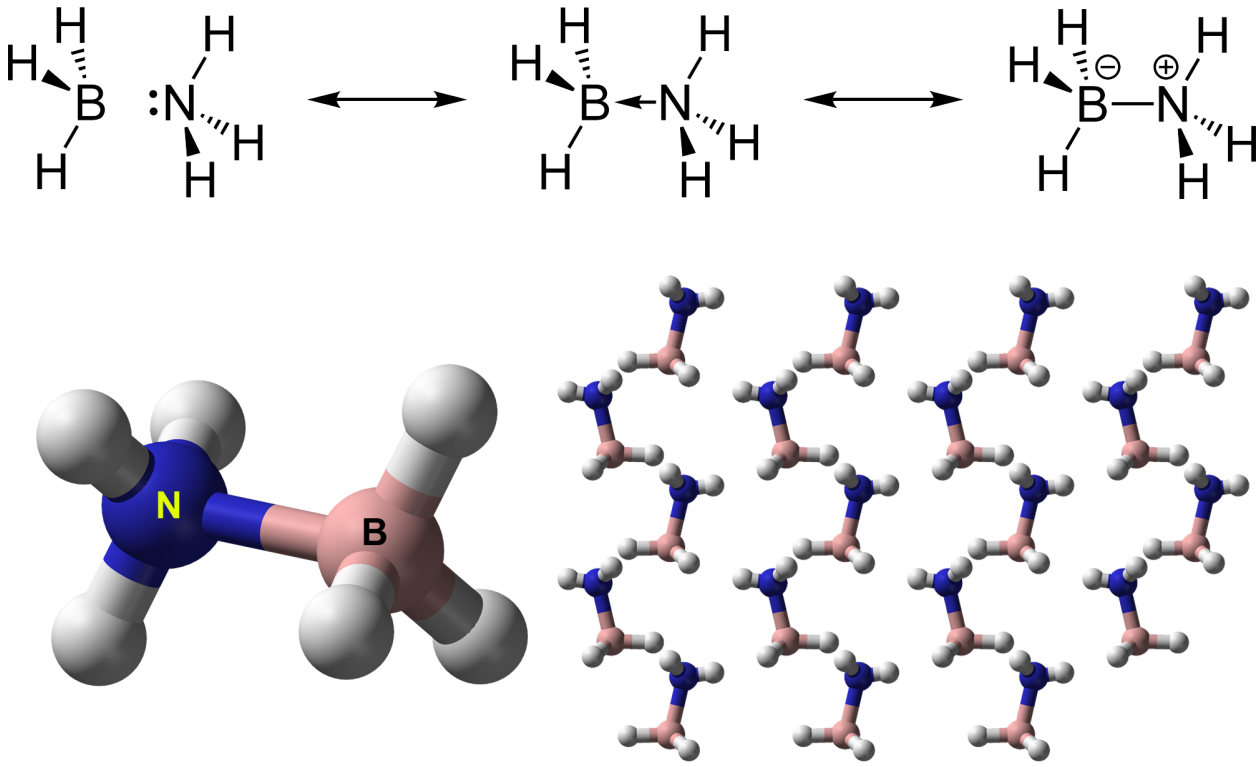

Figure 3: Structure of ammonia borane (HAB). The molecule is a complex of NH_3 and BH_3, with coordination bond between N and B. Hydrogen atoms of the NH_3 are of protic character, while those of the BH_3 group holds a surplus electron density, which makes them hydridic. The two types of hydrogen atoms build dihydrogen bonding network, which stabilizes crystal structure.[75]

In ambient conditions HAB is a white molecular crystal whose unusual properties arise

from the fact that NH_3 and BH_3 are bind by N→B coordination bond (Fig. 3). Even more important is the nature of hydrogen atoms: while NH_3 holds protic $H^{\delta+}$, hydrogen atoms of the BH_3 group are hydride-type $H^{\delta-}$. Thus, HAB represents a combination of Lewis acid ($H^{\delta+}$) and Lewis base ($[NH_2BH_3]^-$). This duality makes them suitable for building $NH^{\delta+}\cdots H^{\delta-}B$ dihydrogen bond network (Fig. 3), which accounts for relatively high melting point (112 °C), while isoelectronic ethane melts at −181.3 °C. Dihydrogen bonding also favorizes release of hydrogen at relatively low temperature, which coincides with melting of HAB.

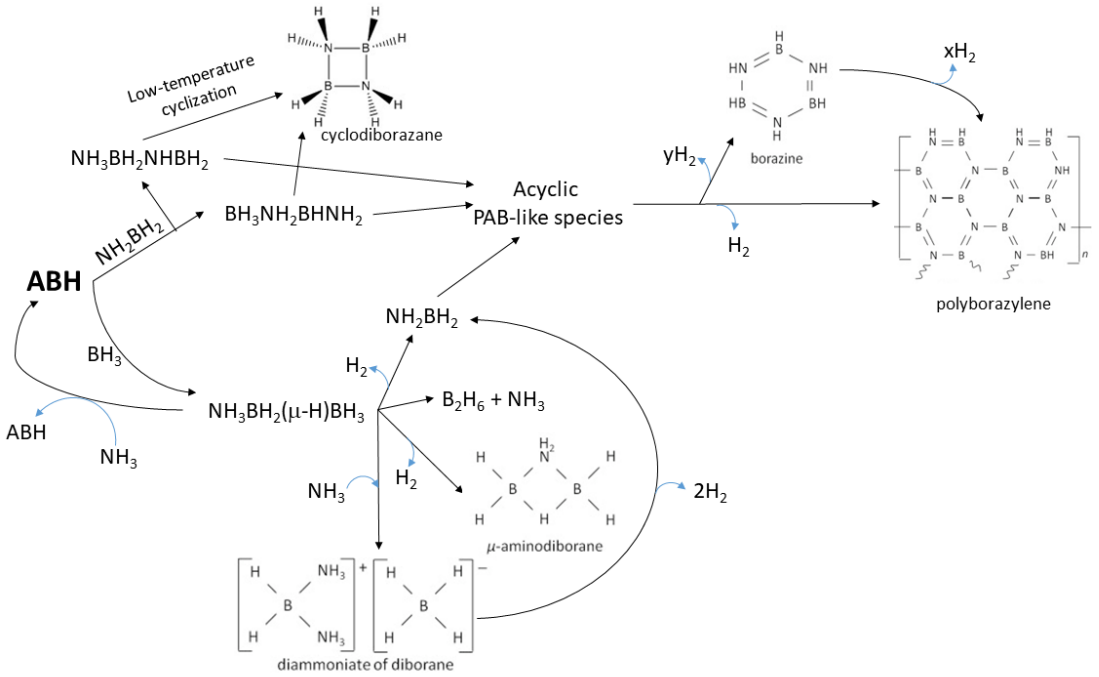

Figure 4: Complex chemistry of the low-temperature step of thermal decomposition of ammonia borane, as proposed by Varma et al.[76] A very complex mixture of various B-N species are formed. Hydrogen is released at several stages of the process, but it is accompanied with release of unwanted ammonia (NH_3), diborane (B_2H_6) and borazine ($N_3B_3H_6$).

However, thermal dehydrogenation of HAB is a very complex process (Fig. 4), which involves formation of various B−N species, NH_3 and diborane, while in the solid state a complex mixture of various stable B−N-containing oligomers and polymers (borazinyl residues, cyclic and cross-linked structures) are formed.[25,76–80] These impurities that accompany re-

leased H_2 make HAB itself incompatible with fuel cells, while its practically unreachable recycling makes it impractical for applications as a source of H_2 in real-world systems.

Due to its high gravimetric and volumetric capacity of hydrogen (19.6 wt.% and 145 g L^{-1}, respectively), as well as stability under ambient conditions, HAB was recognized as one of the most perspective materials for hydrogen storage.[25] However, a sluggish kinetics and unfavourable exothermic thermodynamics remained the major challenges, and finally caused a decrease of research interest, at least in the field of hydrogen storage. For example, Castilla-Martinez et al. argued that this material does not yet have the desired properties for hydrogen storage, but the final verdict can be given after scaling-up studies has been carried out.[33] To the best of our knowledge, no research in this direction has been conducted, probably due to the overall significant drop of interest of the research community in HAB and related materials. However, in recent years HAB and metal amidoboranes (MAB) are also considered as systems expressing high solid-state ion mobility, especially for Mg^{2+},[81,82] which opens the door for their potential application in batteries.

Amidoboranes

Table 1: Basic properties of MABs relevant to hydrogen storage.[30]

Name	**Formula**	Abbreviation	w(H) (wt.%)	t(dehydrogenation) (°C)
Ammonia borane	NH_3BH_3	HAB	19.6	110
Lithium amidoborane	$LiNH_2BH_3$	LiAB	13.5	92
Sodium amidoborane	$NaNH_2BH_3$	NaAB	9.4	89
Potassium amidoborane	KNH_2BH_3	KAB	7.3	80
Rubidium amidoborane	$RbNH_2BH_3$	RbAB	4.4	95
Cesium amidoborane	$CsNH_2BH_3$	CsAB	3.1	105

Single-metal amidoboranes

HAB reacts with metal hydrides giving metallic amidoboranes (MAB), which frequently overcome some of the drawbacks of neat HAB with respect of hydrogen storage. Thus,

they ignited a strong research interest as highly potent candidates for solid-state hydrogen storage, which was undertaken by numerous research groups over the first two decades of this century.[30,31,83–86] Although MABs have smaller gravimetric hydrogen capacity than HAB, it is still high enough for practical applications (over 4.5 wt.% by DOE demands for 2020, see Table 1).[16] Also, hydrogen desorption temperatures of MABs are under 100 °C, which is ideal for hydrogen storage systems coupled with PEM fuel cells, whose working temperature is between $70 - 90\,^{\circ}\mathrm{C}$. A complete series of alkaline metal amidoboranes is exhaustively reviewed by Owarzany et al.[30]

Although the first MAB was reported in 1938,[87] they were inaugurated to the field of materials for solid-state hydrogen storage by Xiong et al. in 2008.[88,89] The authors reported the preparation of lithium and sodium amidoborane (LiAB and NaAB, respectively) by means of ball milling:

$$\mathrm{MH} + \mathrm{NH_3BH_3} \longrightarrow \mathrm{MNH_2BH_3} + \mathrm{H_2} \tag{4}$$

It is interesting to note that the authors observed a significant difference in reactivity of LiH and NaH, respectively, with HAB (Fig. 5). Although they presented data for both systems, NaAB is significantly underrepresented by experimental evidences. For example, the authors claimed that the two systems are isostructural, it is not evident from the present PXRD patterns, while the crystal structure of NaAB was not presented.

Almost simultaneously, Fijalkowski and Grochala reported preparation of NaAB by disk milling.[90] Although the focus of this group was on thermal decomposition of NaAB, its PXRD differs from the one reported by Xiong et al. (Fig. 6). However, these inconsistencies and ambiguities will be discussed further in the text, relying on literature data, as well as our observations about that system.

HAB can be considered as "hydrogen amidoborane" or $\mathrm{H{-}NH_2BH_3}$, making it the simplest representative of MAB family. This review is focused exclusively to s-block MABs, i.e. those composed of IA and IIA group cations and amidoborane anion ($[\mathrm{NH_2BH_3}]^-$).[31] They are mainly interpreted as ionic salts, where metal cations are coordinated by nega-

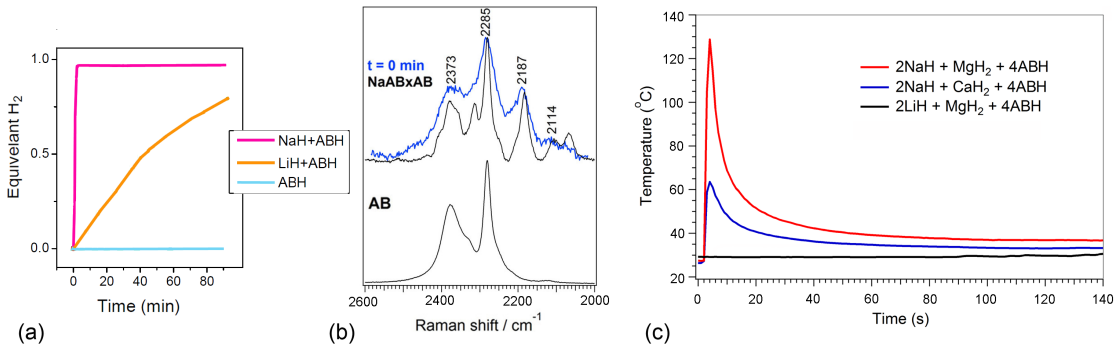

Figure 5: Instantaneous solid-state reaction of NaH with HAB. (a) Mechanochemical reaction of LiH and NaH with HAB, followed by monitoring the pressure of released H_2.[88] (b) Raman spectra of the $2\,NaH + MgH_2 + 4\,HAB$ system show that the product is formed immediately when NaH and HAB are brought to contact, i.e. before the start of milling.[77] Adapted with permission from N. Biliškov et al. *Chem. Eur. J.* **2017** *23* 16274. Copyright 2017 Willey. (c) Temperature monitoring of the ball milling reaction of $2\,M'H + M''H_2 + 4\,HAB$ (M' = Li, Na; M" = Mg, Ca). Untill the start of milling the reagents were kept separated. A steep increase of the temperature is evident at the very start of the milling.[59] Reprinted with permission from I. Milanović et al. ACS Sust. Chem. Eng. **2021** *9* 2089. Copyright 2021 American Chemical Society.

tively charged moieties rather than bonded to nitrogen atom. However, Upon the reaction of NaH with HAB, Na^+ from NaH forms ionic bond with $[NH_2BH_3]^-$ by replacing one protic hydrogen atom with Na^+. One of the protic hydrogens reacts with hydride ion from NaH forming H_2. Actually, there is a competition of $H^{\delta-}$ (from NaH) and $[NH_2BH_3]^-$ ions to establish chemical bond with $H^{\delta+}$ from NH_3 group. Thus, highly Lewis basic MH readily reacts with $H^{\delta+}$ from HAB giving MAB, while weakly basic MH hardly react with HAB. Establishing of ionic bond between alkaline metal and nitrogen contributes the exothermicity of the reaction.[89]

The length of the B−N bond in MABs decreases downward the IA group (Table 2). For RbAB the bond is longer than KAB and continues to decrease downward the group (RbAB > CsAB). So, the influence of alkali metal to the N−B bond is evident from its length.[30,32] This is attributed to stronger bonding between these two atoms in MABs as an effect of hydrogen atom substitution for an alkali metal. As a consequence of electron donating nature of alkali metal, longer M−N bonds in MABs influences the shortening of N−B bonds. These experimental results are supported by calculated lengths of N−B and

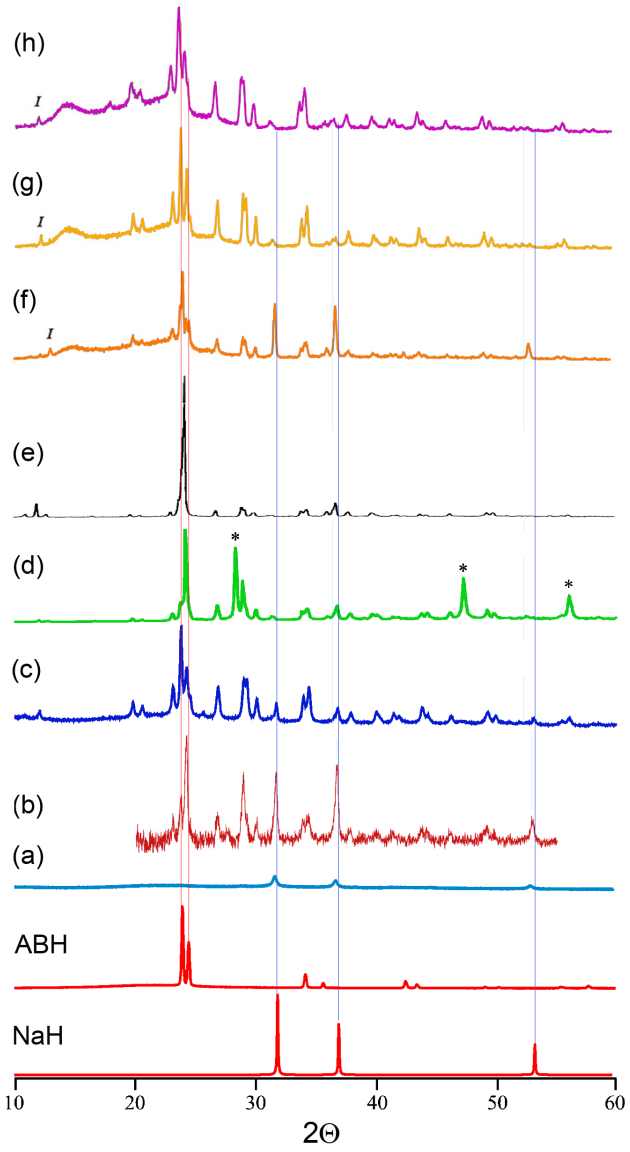

Figure 6: PXRD patterns for the NaH+HAB subjected to different preparational treatments leading to NaAB: (a) ball milling in stainless steel jar; (b) the same as (a), but with pre-treated HAB;[91] (c) disc milling;[90] (d) ball milling in stainless steel jar (* denotes Si added as standard);[88] (e) THF solution;[89] (f) ball milling in stainless steel jar;[92] (g) manual grinding in mortar with pestle;[92] (h) mixing with spatula.[92] PXRD for NaH, HAB and a measured by the authors. *I* in f-h denotes the line due to the kapton tape used to protect the sample from air. Blue and red lines indicate the positions of the lines due to remaining NaH and HAB, respectively.

M−N bonds (Table 2).

The N−H bond is not significantly affected by substitution of hydrogen with alkali metal (Table 2). Experimental values of N−H bond length for RbAB and CsAB compounds are unknown.[30] On the other hand, substitution of H with M significantly affects B−H bond, which enhances its hydridic character. This directly influences dehydrogenation characteristics,[93] since the amplified hydride reacts more readily with protic hydrogen $H^{\delta+}$ of the NH_3 moiety. Autrey et al. have shown that in MABs generation of M−H bond through metal ion-assisted hydride transfer is a rate determining step of the process of dehydrogenation.[94] Computational analysis of dehydrogenation process shows that this is a two-step process.[95] The highest free energy barrier originate from transition state which includes Li−H···H−Li interaction. Thus hydrogen desorption from MABs represents superposition of two main interactions, $BH^{\delta-}\cdots M^{+}$ and $BH^{\delta-}\cdots H^{\delta+}N$. As a consequence, dehydrogenation energies of MABs are decreased with respect to HAB (Table 1). The other contributions does not significantly affect dehydrogenation of MABs.

The length of intermolecular $H^{\delta+}\cdots H^{\delta-}$ distance is directly correlated to alkali metal.[100,105] Substitution of one hydrogen with alkali metal leads to increase of this contact from 2 Å to $\sim$ 2.7 Å and 2.26 Å for KAB, which is caused by the different coordination geometry (Table 2). It is indicative that the longest $H^{\delta+}\cdots H^{\delta-}$ distance is observed for NaAB, which directly leads to its instability. The length of dihydrogen bonding contact in this system is higher than the sum of van der Waals radii of the two hydrogen atoms (> 2.4 Å). The $H^{\delta+}\cdots H^{\delta-}$) for KAB is shorter than expected due to the change of cation coordination from tetrahedral in NaAB and LiAB to octahedral geometry. This change of geometry is caused by increased packing density of the $[NH_2BH_3]^-$ anions,[100] and it influences the hypothesized homopolar $BH^{\delta-}\cdots H^{\delta-}B$ (hydride-hydride) and $NH^{\delta+}\cdots H^{\delta+}N$ (proton-proton) interactions.[106] On the basis of theoretical considerations, Wolstenholme et al. concluded that hydride-hydride interactions are surprisingly strong and play a substantial role in solid state structural stabilization of MABs.[106]

Table 2: Bond lengths for ammonia borane and metallic amidoboranes.

Compound (abbreviation)	**Bond**	**Bond length /Å**		**Reference**
		Experimental	**Calculated**	
NH_3BH_3 (HAB)	N−B	1.56; 1.58	1.5978	[96–98]
	N−H	1.03; 1.07	1.0291	[96,97,99]
	B−H	1.18; 1.21	1.2220	[96,97]
	intermol. $H^{\delta+}\cdots H^{\delta-}$	1.96; 2.03; 1.7-2.2	2.2012	[96,99,100]
$LiNH_2BH_3$ (LiAB)	N−B	1.561	1.547	[101]
	Li−B	2.51 − 2.97	2.50 − 2.69	[101]
	N−H	1.025; 1.025	1.2220	[101]
	B−H	1.249	1.244	[101]
	Li−N	2.032; 1.98	2.063	[89,101]
	intermol. $H^{\delta+}\cdots H^{\delta-}$	2.717	—	[100]
$NaNH_2BH_3$ (NaAB)	N−B	1.56	1.59	[89,102]
	Na−B	2.68 − 2.93	2.823 − 2.899	[102,103]
	N−H	1.04 − 1.05	1.02	[102,103]
	B−H	1.29 − 1.32	1.21; 1.25	[102,103]
	Na−N	2.14; 2.35	2.26	[89,102,103]
	intermol. $H^{\delta+}\cdots H^{\delta-}$	2.717	—	[100]
KNH_2BH_3 (KAB)	N−B	1.53	1.542; 1.544	[100,104]
	K−B	3.28 − 3.59	—	[100]
	N−H	0.78 − 1.05	1.027(N1); 1.026(N2)	[100,104]
	B−H	1.08 − 1.26	1.238; 1.239; 1.255(B1)	[100,104]
	K−N	3.0207 − 3.1345;2.91 − 3.36	2.980; 3.053; 3.173	[100,104]
	intermol. $H^{\delta+}\cdots H^{\delta-}$	2.2650	—	[100]
$RbNH_2BH_3$ (RbAB)	N−B	1.56(2)	1.548	[105]
	Rb−B	3.191(18)	3.216	[105]
	N−H	—	—	—
	B−H	—	—	—
	Rb−N	3.06(1)	3.016	[105]
	intermol. $H^{\delta+}\cdots H^{\delta-}$	—	> 2.3	[105]
$CsNH_2BH_3$ (CsAB)	N−B	1.54(2)	1.539	[105]
	Cs−B	3.67(3)	3.254	[105]
	N−H	—	—	—
	B−H	—	—	—
	Cs−N	3.281(13)	3.173	[105]
	intermol. $H^{\delta+}\cdots H^{\delta-}$	—	> 2.3	[105]

Van der Waals interaction between M^+ and the three closest BH_3 units additionally stabilizes the structure.[106] This $BH^{\delta-}\cdots M^+$ interaction plays a similar stabilizing role in MABs like dihydrogen bonding in HAB. This interaction gives enough energy to MNH_2NH_3 to remain solid and stable at room temperature.[100]

Sodium Amidoborane - a Special Case

Obviously, hydrogen capacity of HAB and LiAB is higher with respect of NaAB, and they attracted a significantly more research attention.[28,30] However, some properties of NaAB make it potentially even more interesting for hydrogen storage. This is especially valid for relatively low dehydrogenation temperature, fast dehydrogenation kinetics and in some cases reported emission of pure H_2 (Table 4). However, relatively high sodium ion mobility[107] and as a consequence a substantial difference of its dehydrogenation pathway with respect to LiAB,[108] altogether make its thermal dehydrogenation especially complex, even with respect to other members of its closer amidoborane or wider family of complex hydrides, although the final dehydrohgenation products are common for all amidoboranes (BN and often NH_3 and borazine). Such a complexity of dynamics and dehydrogenation pathways make NaAB a special case among other amidoboranes.

As mentioned earlier, sodium amidoborane is the first reported member of the entire family of amine boranes. It was prepared by Schlesinger and Burg in 1938[87] by reaction of etherate $(CH_3)_2OBH_3$ with sodium in liquid ammonia:

$$Na + (CH_3)_2OBH_3 + NH_3 \longrightarrow NaNH_2BH_3 + (CH_3)_2O + \frac{1}{2}H_2 \qquad (5)$$

and named the product sodium amidotrihydroborate. That publication attracted just a very limited interest, exclusively in the context of comparison with other boron compounds. NaAB itself did not appear again in the literature until 2008, when Xiong et al. have reported its mechanochemical synthesis in two subsequent publications,[88,89] which was readily

followed by Fijalkowski et al.[90] and other authors.[30,91] NaAB is today usually synthesized from reaction of NaH with HAB in THF solution or mechanochemically.

Table 3: Crystal structure parameters of LiAB and NaAB.

		space group	a(Å)	b(Å)	c(Å)	V(Å^3)	Ref.
LiAB	α	*Pbca*	7.11	13.93	5.15	509.5	[109]
	β	*Pbca*	15.15	7.72	9.27	1083.8	[109]
NaAB	Xiong	*Pbca*	7.46931(7)	14.65483(16)	5.65280(8)	618.764(20)	[89]
	Ryan	*Pbca*	7.4680(16)	14.6474(32)	5.6548(9)	618.56	[103]
	Ramzan	*Pbca*	7.46931	14.65483	5.65280	618.764	[110]

NaAB is an off-white crystalline powder, stable when stored in argon atmosphere for a few days.[90] It crystallizes in orthorhombic system (Table 3, Fig. 7).[89,103] The results obtained by calculation[110] are in very good agreement with experimental values.[89,103] The highest deviation is caused by different B-N distences as obtained by Ryan (d(B−N) = 1.670 Å)[103] and Xiong et al. (1.56 Å),[89] which is unreasonable since B−N bond length difference between other alkali metal amidoboranes is much smaller.[89,101] Wu et al. have justified that α-LiAB and NaAB are isostructural.[101] In crystal, Na^+ is surrounded by 4 $[NH_2BH_3]^-$ groups in tetrahedral coordination (Fig. 7). Na−N bonding is of ionic character. Also, the Na···BH coordination is an evident structural motif (Fig. 7).[89,106]

With practical gravimetric hydrogen capacity of 7.4 wt.% and hydrogen desorption temperature of 91 °C, NaAB was recognized as a very prominent candidate for replacement of magnesium hydride (MgH_2). If we merely compare H_2 desorption temperature of 420 °C for MgH_2 with 91 °C for NaAB and quite the same gravimetric capacity (7.7 wt.% for MgH_2), one could conclude that NaAB is exactly what researchers were looked for.[51] However, the available literature on NaAB brings contradictory evidences on side-emission of NH_3 and other species together with H_2 upon its thermal dehydrogenation.[90,92] Additionally, similar to HAB, NaAB does not meet practical reversibility by rehydrogenation, which is one of the most important requirements for utilization of the material for practical hydrogen storage. This is a consequence of high reactivity of NaAB and very stable solid-state products of its

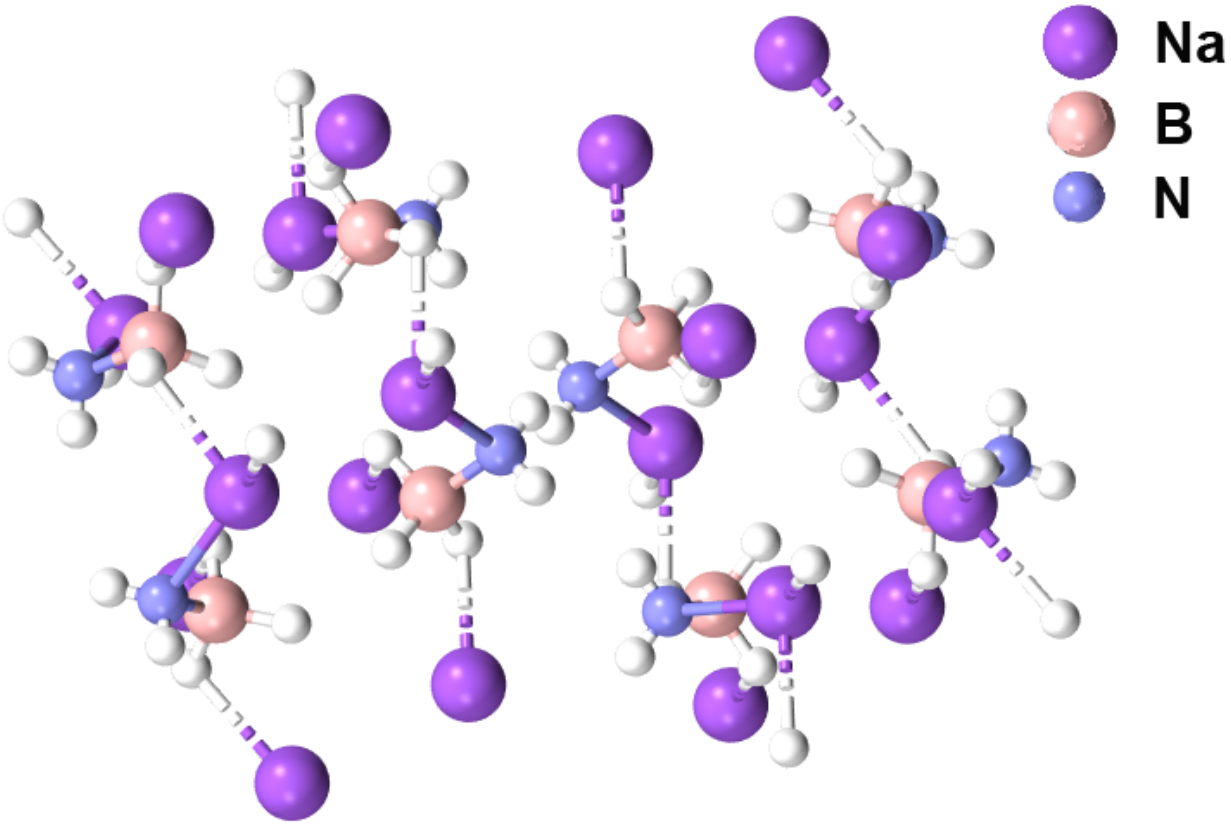

Figure 7: Crystal structure of NaAB. Na^+ is bound to N by replacing a protic H, and it is additionally stabilized through $Na^+ \cdots H^{\delta-}B$. Reprinted with permission D. J. Wolstenholme et al. *J. Amer. Chem. Soc.* **2011** *133* 16598. Copyright 2011 American Chemical Society.

dehydrogenation. Thus, a series of publications that appeared between 2009 and 2015 have revealed increased reactivity of NaAB and possibilities to form different metal amidoborane-like compounds in dependence of temperature and reactants ratio of starting mixture.

In the last few years, the research interest for NaH-HAB system switched from hydrogen storage to potential applications which were made possible by considering other properties of that system. For example, NaAB shows chemically driven negative linear compressibility.[111] Also, Brønsted and Lewis base behavior of NaAB is investigated for potential applications in different organic and inorganic reactions.[112] Finally, in line with the investigation of NaAB as sodium ion conductor,[107] a relatively fast solid-state diffusion is evident for NaH-HAB system, which opens a possibility for application of this system in innovative sodium battery concepts. Isothermal electric impedance spectroscopy (EIS) of NaAB and LiAB shows a faster growth of ionic conductivity at elevated temperatures, with a characteristic maximum of growth rate,[107] which indicates that a competition of thermally-iduced multiplication of charge carriers and a drop of ionic species due to thermally-induced decomposition of NaAB takes place.

Synthesis of NaAB

The first reported synthesis of NaAB represents an example of solution-phase reaction,[87] but this approach was not utilized later. Typically THF is used as a solvent:[32,88,113]

$$\mathrm{NH_3BH_3 + NaH \xrightarrow{THF} NaNH_2BH_3 \cdot THF + H_2(g)} \tag{6}$$

This reaction is first reported by DeGrafenried and it was performed in liquid NH_3 at $-78\,^{\circ}\mathrm{C}$.[113] However, it is observed that the solvent strongly coordinates the product, so it crystallizes as solvate.[114,115] Xiong et al. synthesized NaAB by reaction between $NaNH_2$ and HAB at $25\,^{\circ}\mathrm{C}$.[88] The reaction mixture was stirred for 20 h until the constant pressure

in reactor was reached. During the reaction, ammonia is evolved:

$$NH_3BH_3(sol) + NaNH_2(s) \xrightarrow{THF} NaNH_2BH_3(sol) + NH_3(g) \tag{7}$$

Emmision of NH_3 is a consequence of metathesis reaction between sodium ion on amide and hydrogen ion on HAB. Distillation of $NaNH_2BH_3 \cdot THF$ lead to removal of solvent and formation of $NaNH_2BH_3$. MABs can also be obtained through reactions of HAB with imides and nitrides.[32] Metathesis could also be used for production of new metal amidoboranes:[116]

$$M'X + M''AB \longrightarrow M'AB + M''X \tag{8}$$

This method is applied to prepare alkaline earth metal amidoboranes or transition metal amidoboranes.

Less frequently used methods for synthesis of NaAB sporadically appear in the literature. For example, Shore and Perry prepared NaAB from elemental sodium and HAB in liquid ammonia at $-78\,^{\circ}C$, which results in release of 1/2 equivalent of H_2:[117]

$$Na + NH_3BH_3(s) \longrightarrow NaNH_2BH_3(s) + \frac{1}{2}H_2(g) \tag{9}$$

They did not isolated and analysed the obtained product. DeGrafenried reported reaction between HAB and alkyl-sodium:[113]

$$RM + NH_3BH_3 \longrightarrow MNH_2BH_3 + RH \tag{10}$$

This reaction was performed in THF solution at $0\,^{\circ}C$ with slow addition of reactants. Main drawback of this approach is formation of alkylated derivates of HAB as side-products.

Mechanochemistry, most usually ball milling, is frequently used to obtain NaAB and

other MABs:[89–91,118]

$$NH_3BH_3(s) + NaH(s) \xrightarrow{\text{ball milling}} NaNH_2BH_3(s) + H_2(g) \quad (11)$$

This reaction is inherently solid state. Although the authors claimed that this reaction results in pure NaAB, making this approach the method of choice,[114,119] our experience shows that it only rarely leads to a mixture of the product and NaH and HAB rather than pure NaAB. Additional benefit of the mechanochemical approach lies in the very fact that solvents are absent, which makes it aligned with principles of green chemistry.[120] Although ball milling is the most popular mechanochemical method, disc milling[30] and hand grinding in mortar with pestle[91,92] are also present in the literature. A drawback of this synthesis approach in the case of NaAB is its high sensitivity to various, hardly controllable parameters, which makes its outcome highly unpredictable. For example, some salts related to NaAB, such as $[Na]^+[BH_3NH_2BH_3]^-$, were not mechanochemically synthesized for a long time.[30]

At this point, it is worth to look back again at the seminal publications by Xiong et al.[88,89] To synthesize NaAB, they employed a planetary mill at 200 r.p.m., and unspecified amount of graphite was added to reaction mixture consisting of NaH and HAB in equimolar amount.[88] Mass of the balls and reaction time are not specified. However, as shown in Fig. 5, 1 equivalent of H_2 is released instantly upon the very start of milling, which indicates an extremely fast reaction. The same group reported the reaction of NaH and HAB in THF.[89] PXRD pattern of the product differs in several lines and intensities to that obtained by ball milling (Fig. 6). Following these publications, Fijalkowski reported preparation of NaAB by disc milling.[90] Although the authors indicate unreacted NaH, their PXRD again clearly differs from the one reported by Xiong. Sandra et al. compared NaAB prepared by three different low-energy mechanochemical methods.[92] They applied a homogenizer to perform low-energy ball milling, manual grinding in mortar with pestle and simple mixing of the reagents by spatula. Although their results show that NaAB is obtained by all the applied

methods, their PXRD patterns show that among the three methods ball milling was least efficient by means of achieved conversion of NaH and HAB to NaAB.

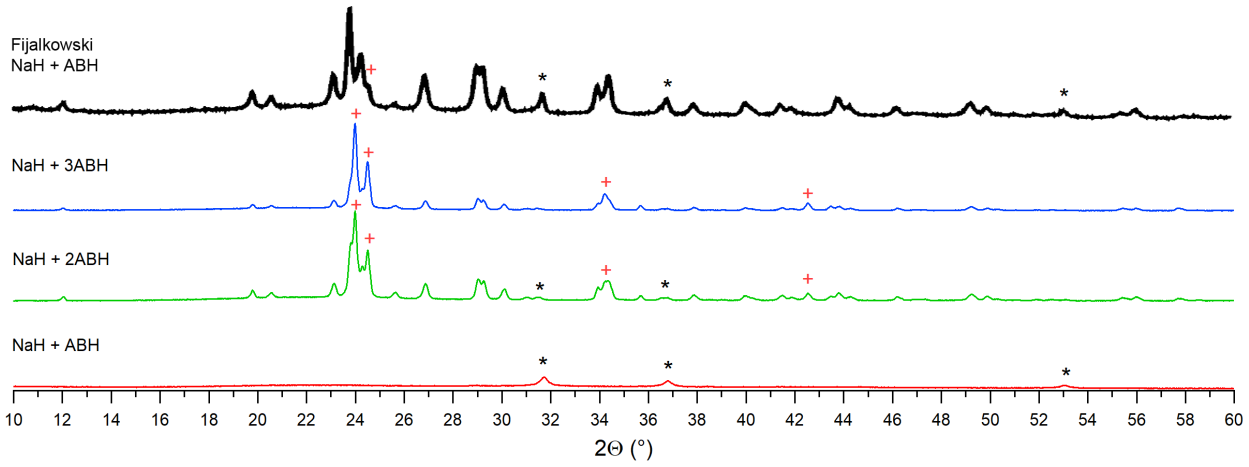

Figure 8: PXRD patterns of the products of NaH + xHAB ($x = 1$, 2, 3) ball milling reactions (performed by the authors), as compared to the product obtained by disc milling.[90] Symbols * and + denote NaH and HAB lines, respectively.

We have performed a series of mechanochemical reactions of the NaH + xHAB ($x = 1-3$, Figs. 8 and 9). For this purpose, we used a Spex 8000M mill-shaker, which agitates the vial at a high frequency in a complex three-axis cycle. The center of vial vibrates in 2D mode with the same frequency, but with different amplitude. The main axis of the vial is slanted and it rotates (at the same frequency) around the axis of precession. A 250 mL cilindrical stainless steel jar with $2 \times 3\,\mathrm{g} + 2 \times 1.3\,\mathrm{g}$ balls were used. For comparison, the reaction was also performed in a smaller milling 14 mL vial with one 3 g stainless steel ball. As expected, outcome of the reaction depends on molar ratio of the reagents. The results are shown in Figs. 8 and 9.

Different to previously reported results,[88,90] here performed milling of the equimolar mixture of NaH and HAB results in amorphous product. When performed in a bigger jar, the product is a grey paste, which IR spectrum indicates extensive decomposition (Fig. 9), while PXRD shows some remaining NaH, with no traces of HAB or any crystalline product (Fig. 8). When performed in smaller jar, the reaction results in an amorphous, deep violet coloured powder, which was not previously reported.

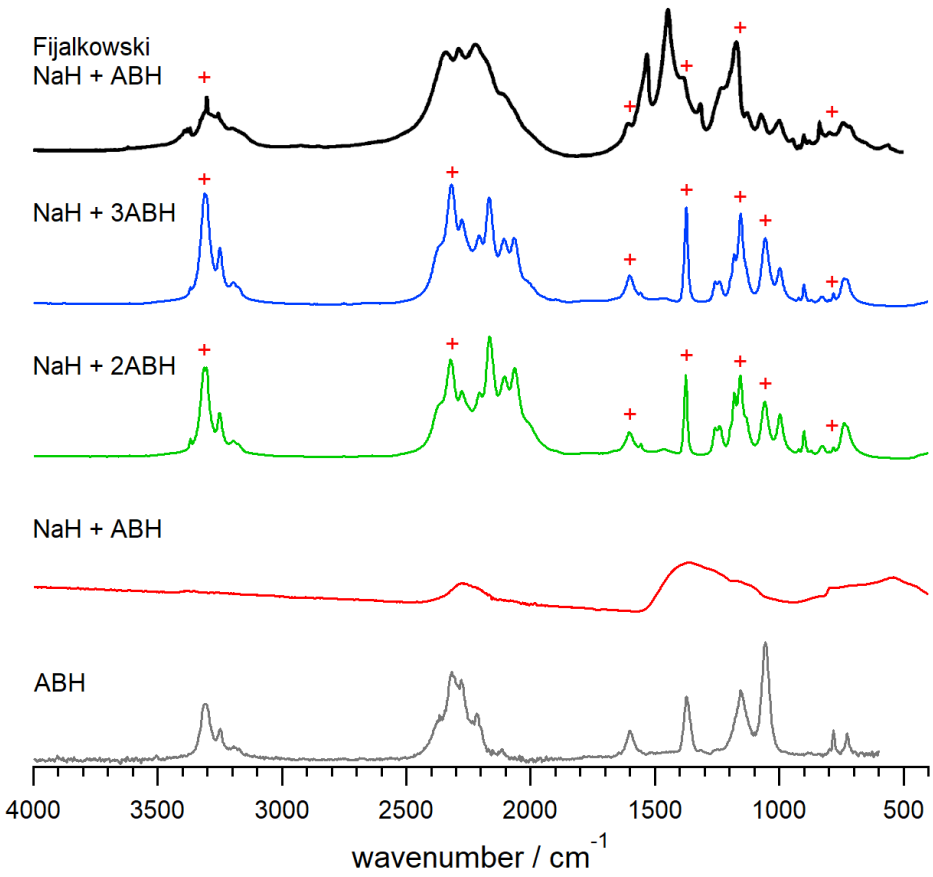

Figure 9: IR spectra of the products of NaH + xHAB (x = 1, 2, 3) ball milling reactions (performed by the authors), as compared to the product obtained by disc milling.[90] Symbol + denotes HAB bands.

Temperature monitoring of the systems involving NaH and HAB mixture systems shows an abrupt and very intense temperature increase in the first seconds of the milling (Fig. 5(c)), which results in formation of (previously unreported) deep violet amorphous product, which contains $NaBH_4$.[59] Additionally, Xiong et al. have observed a very fast increase of partial pressure of H_2, which reaches 1 equivalent in the first few seconds of the milling (Fig. 5(a)), indicating a very violent reaction between NaH and HAB.[88] Sandra et al. applied low-energy milling conditions, and they show that the amount of remaining NaH is opositely correlated to the input energy. Their product obtained by ball milling contains a substantial amount of unreacted NaH, while manual grinding and especially simple mixing of the mixture by spatula resulted in product in which only traces of NaH are visible.[92] This is in line with our observation that the product is formed immediately by bringing NaH and HAB to contact.[77]

All the above mentioned observations indicate a relatively fast diffusion in the NaH+HAB system. Being extremely exothermic, the reaction causes overheating of the system and decomposition of unreacted HAB and the formed product. Larger stainless steel milling jar enables a more efficient heat removal and thus partial cooling of the reaction mixture. On the other hand, smaller vials or PMMA vials are not so efficient in this regard, and the reaction ends up in (previously unreported) deep violet $NaBH_4$ containing product. The occurence of the pasteous product in the case of larger jar indicate the formation of eutectic liquid intermediate which could facilitate diffusion in this system. These hypotheses should be experimentally justified.

The first possible outcome of the NaH+2 HAB reaction would be the adduct $NaAB \cdot HAB$, which is formed with evolution of 1 equivalent of H_2. The production of adduct is observed for the analogous system $LiH + 2\,HAB$:[109]

$$LiH + HAB \longrightarrow LiAB + H_2 \tag{12}$$

$$LiAB + HAB \longrightarrow LiAB \cdot HAB \tag{13}$$

Production of this adduct is confirmed by monitoring the reactions involving LiH and HAB in 1 : 2 molar ratio, involving the synthesis of mixed lithium-alkaline earth amidoboranes.[59,77] LiAB · HAB represents a general intermediate in reactions involving LiH and HAB, where in the first step LiAB · HAB is formed, while in the second step the adduct reacts with LiH (in the case of LiH : HAB = 1 : 1) giving LiAB or with another present hydride (Figs. 10, 8 and 9).

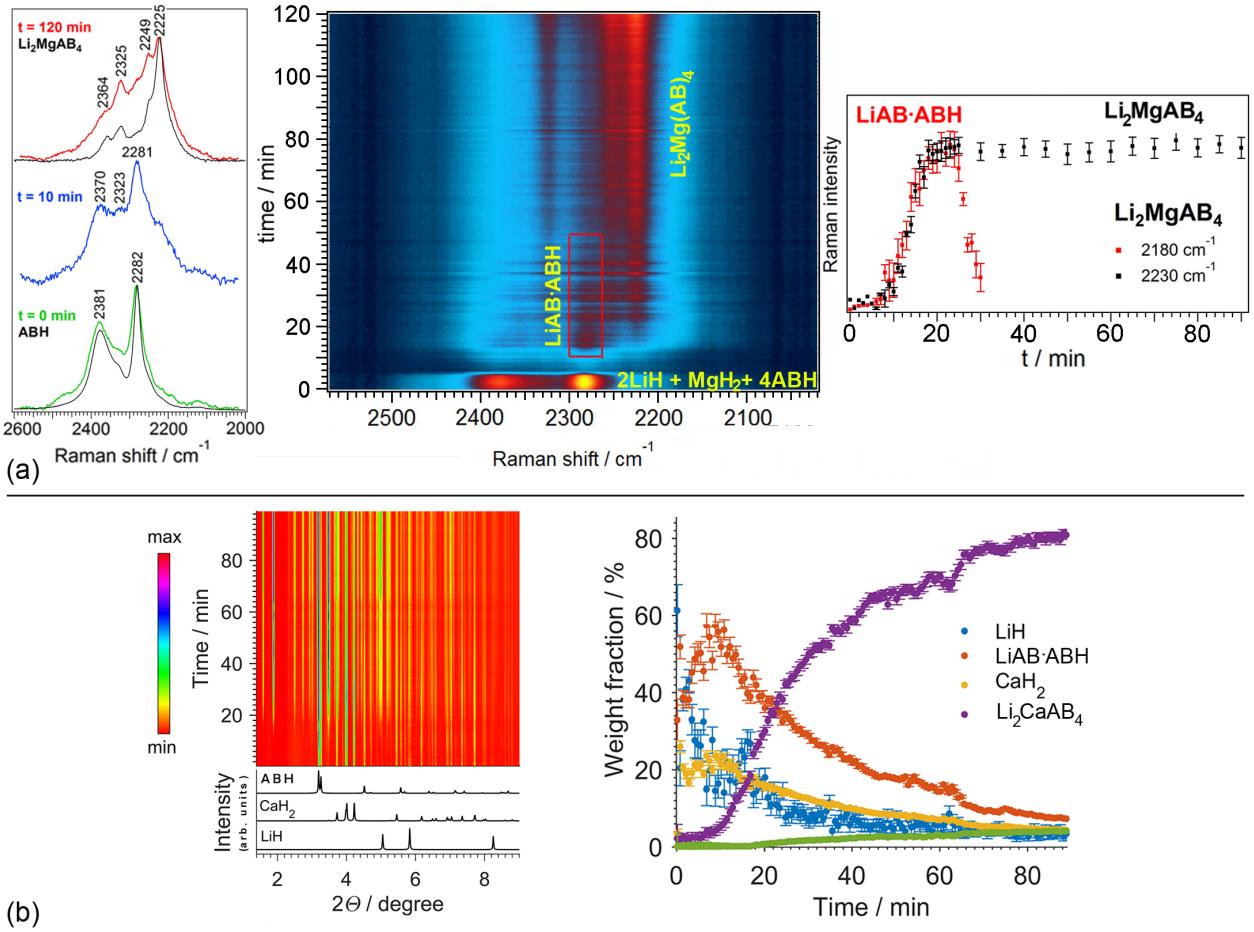

Figure 10: Mechanochemical synthesis of bimetallic Li-containing amidoboranes: (a) $Li_2Mg(AB)_4$, as monitored by Raman spectroscopy. Extracted spectra at different times show reagents (HAB spectrum), intermediate adduct LiAB · HAB and final product, which is additionally indicated by reaction profile;[77] Adapted with permission from N. Biliškov at al. *Chem. Eur. J.* **2017** *23* 16274. Copyright 2017 Willey. (b) $Li_2Ca(AB)_4$, as monitored by synchrotron PXRD and extracted reaction profile, which again indicates intermediate adduct LiAB · HAB.[59] Reprinted with permission from I. Milanović et al. *ACS Sust. Chem. Eng.* **2021** *9* 2089. Copyright 2021 American Chemical Society.

However, mechanochemical reaction NaH+2 HAB results in the same product as obtained

by Fijalkowski[90] and Sandra,[92] in both cases attributed to NaAB. As evident from the Fig. 6, PXRD of the product is equal to those reported by these authors for 1 : 1 system.

Another possible pathway of the NaH + 2 HAB reaction leads to $NaBH_3NH_2BH_3$ with evolution of 1 equivalent of NH_3 and H_2. In the first step, NaAB phase is formed with release of 1 equivalent of H_2 (equation 11), while in the second step NaAB reacts with remaining 1 equivalent of HAB, which results in $Na(BH_3NH_2BH_3)$ (sodium aminodiboranate or NaADB) and evolution of NH_3:

$$NaNH_2BH_3 + NH_3BH_3 \longrightarrow NaNH_2(BH_3)_2 + NH_3(g) \tag{14}$$

Formation of NaADB is for the first time reported in 2010 by Davy et al.[114] and later by Chen et al.[121] However, it is evident that Schlesinger et al. very probably also obtained NaADB,[87] but at this time it was impossible to resolve its structure. They studied reaction of sodium with solution of the diammoniate of diborane ($B_2H_6 \cdot 2\,NH_3$, DADB) in liquid ammonia. Their experiment where "quantity of sodium was just one equivalent per mole of diborane" resulted in a stable salt with empirical formula NaB_2H_8N. They also observed release of H_2 during the reaction:

$$B_2H_6 \cdot NH_3 + Na \longrightarrow NaB_2H_8N + NH_3(g) + \frac{1}{2}\,H_2 \tag{15}$$

By comparing the reactions (11) and (10)[87] it is evident that $B_2H_6 \cdot 2\,NH_3$ empirically corresponds to $2\,NH_3BH_3$, while NaB_2H_8N corresponds to $Na(BH_3NH_2BH_3)$. Additionally, Evans described a spontaneous nature of the reaction of NaAB with itself and reaction between HAB and NaAB.[122] In both cases the NH_2^- anion (nucleophile) attacks the B atom of HAB or NaAB, which causes removal of the proton from NH_3 group and formation of new N−B bond:

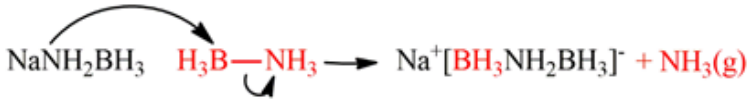

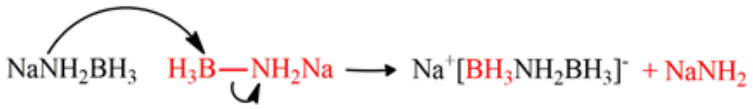

Evans did not solve the crystal structure of $Na^{+}(BH_3NH_2BH_3)^{-}$ phase, which is later done by Fijalkowski et al., showing that it is actually $Na(BH_3NH_2BH_2NH_2BH_3)$ phase (further in the text denoted as NaB3N2). Thus, it seems that the reaction $NaH + 2\,HAB$ and $NaH + 3\,HAB$ in THF result in the same product. Above 110 °C $Na(BH_3NH_2BH_2NH_2BH_3)$ phase decomposes to $NaBH_4$:

$$Na(BH_3NH_2BH_2NH_2BH_3) \longrightarrow NaBH_4 + 2/\,n(NHBH_n + 2\,H_2 \tag{16}$$

Another important observation in the case of 1 : 2 ratio is increase of NaAB : HAB ratio with temperature, which is followed by appearance of trails of trigonal NaB3N2 phase.[122] As discussed earlier, NaB3N2 phase is dominant between 60 and 110 °C, without detectable presence of NaAB and HAB.

Girolami et al. reported synthesis of NaADB by reaction of Na with HAB in THF at room temperature,[114] justifying the formation of B−N−B bridge with N-alkyl analogues:

$$4\,HNRR' \cdot BH_3 + 2\,Na \longrightarrow 2\,Na(BH_3{-}NRR'{-}BH_3) + H_2 + 2\,HNRR' \tag{17}$$

The same product was obtained by reaction of 2 equivalents of HAB with $NaNH_2$ in THF reflux, through intermediate NaAB.[114] This outcome was later confirmed by two different groups.[121,123]

It is evident that the outcome of the $NaH + 2\,HAB$ reaction differs for the mechanochemical approach with respect of the solution reactions. Thus, it would be interesting to monitor liquid-assisted mechanochemical reaction, where the catalytic amount of the liquid is added to the system.

The result of the mechanochemical reaction of the system $NaH + 3\,HAB$ is equal to

the above discussed NaH + 2 HAB with more unreacted HAB remaining in the mixture, as evident from Figs. 8 and 9.

Reaction in THF solution results in a product whose formation is accompanied with release of H_2 and NH_3:

$$NaH + 3\,NH_3BH_3 \longrightarrow Na(BH_3NH_2BH_2NH_2BH_3) + 2\,H_2(g) + NH_3(g) \tag{18}$$

The NaB3N2 phase is identified by Fijalkowski et al.[124,125] Additionally, the authors observed formation of the NaB3N2 by thermal rearrangement of NaAB at 50 °C:

$$2\,NaNH_2BH_3 \xrightarrow{\Delta} [Na(NH_3)](BH_3NH_2BH_2NH_2BH_3) + 2\,Na \tag{19}$$

$$[Na(NH_3)](BH_3NH_2BH_2NH_2BH_3) \longrightarrow Na(BH_3NH_2BH_2NH_2BH_3) + NH_3 \tag{20}$$

This process is actually more complex. Fijalkowski et al. hypothesized a reaction pathway:[124]

$$5\,Na(NH_2BH_3) \longrightarrow [Na(NH_3)](BH_3NH_2BH_2NH_2BH_3) + 2\,Na_2(NHBH_3) + H_2 \tag{21}$$

However, this is not experimentally justified. Further heating of NaB3N2 leads to $NaBH_4$ through (16),[122,124] which explains evidence of formation of BH_4^- ions in some cases.[59]

Above 200 °C $(NHBH)_n$ decomposes to BN:

$$1/\,n(NHBH)_n \longrightarrow BN + H_2 \tag{22}$$

Computation of the hydrogen release enthalpy by dehydrogenation of $M(NH_2BH_3)_n$:

$$M(NH_2BH_3)_n \xrightarrow{\Delta} MH_n + nBN + 2\,nH_2 \tag{23}$$

gives significantly higher exothermic values with respect of those measured experimentally,[126] which indicates a different mechanistic pathway. The proposed alternative mechanistic path-

way that involves monomerica and polymeric $[NHBH_2]^-$, $[NBH]^-$, $[N_3BH_2B_3H_3]^-$ species was also excluded by further DFT considerations, but they indicated a pathway involving $[NHBHNHBH_3]^{2-}$.[127] These calculations also show that alkaline amidoboranes become more stable with respect to dehydrogenation with increasing electropositivity of the metal cation (Li $\longrightarrow$ Na $\longrightarrow$ K), and alkaline earth amidoboranes more readily dehydrogenate with respect to their alkaline counterparts (stability increases in order Ca $\longrightarrow$ K).[127]

To conclude, NaH reacts with HAB in different ways, which depends on the reaction medium, heat transfer and other parameters. The outcome of the solution-phase reaction of NaH with HAB depends on NaH : HAB ratio. Mechanochemical reactions strongly depend on heat transfer from the reaction mixture, which is especially dramatically evident for 1 : 1 system, while 1 : 2 and 1 : 3 systems result in adducts, with remaining unreacted HAB, especially in the 1 : 3 case (Figs. 8 and 9). From the practical point of view, such a rich variability of reaction outcomes and its high dependence on numerous parameters makes the NaH + nHAB system very hard to control, which in turn makes it highly impractical for real world applications.

Hydrogen desorption

HAB desorbs hydrogen in two steps at 108 and 154 °C (Table 4).[50,80] Substitution of protic hydrogen with Na^+ causes a decrease of the temperature of the first dehydrogenation step to 89 °C (Table 1), while the second dehydrogenation step is observed over the $140 - 220$ °C range (Fig. 11, Table 4).[92,107] Decrease of the temperature of the first dehydrogenation step of NaAB is a consequence of previously discussed differences in bonding, i.e. Na−N interaction which strengthens N−B bond stronger with simultaneous weakening of the B−H bond (Table 2), which consequently promotes dehydrogenation.

Two possible mechanistic pathways for pyrolitic dehydrogenation of alkali amidoboranes through a formation of dihydrogen bonds are proposed based on DFT calculations.[128] The first involves NH···HB and the other MH···HB dihydrogen bonding. DFT confirmed a sig-

nificantly lower energy barrier for formation of MH···HB pair, consequently promoting dehydrogenation in alkali amidoboranes with respect of HAB. Additionally, the calculation indicates the highest dehydrogenation rate for NaAB over a family of alkali amidoboranes. A theoretical recondsidearation of the high-pressure and pyrolytic experiments have reveal a crucial role played by dihydrogen bonding interaction in dehydrogenation alkali metal amidoboranes.[108,111] Starting from the observation that dihydrogen bonding network, generally present in alkali amidoboranes, causes shift of spectral absorptions toward both lower and higher wavenumbers indicate a high hydrogen bonding-driven hydrogen mobility in these systems, which is further promoted by heating. Such a high ion mobility induces endothermic melting of crystal lattice which precedes decomposition, which can be a vigorous process, which is the case for NaAB.[111] It is interesting to note that melting temperatures, predicted here, increase in the sequence KAB < NaAB < LiAB. Such a relatively high melting temperature for LiAB indicate a mechanistic pathway different than the one explaining dehydrogenation of higher alkali amidoboranes. Consequently, this indicates that the findings on the trimerization of LiAB,[129] as an intermediate state during the dehydrogenation of this system, cannot be applied to NaAB.

PXRD shows that NaH persists as the only crystalline species in amorphous matrix after decomposition of NaAB, which indicates a similar decomposition product as in the case of HAB (Table 4).[89,122] The first dehydrogenation step was interpreted as:

$$\mathrm{nNaNH_2BH_3} \longrightarrow (\mathrm{NaNHBH_2})_\mathrm{n} + \mathrm{nH_2(g)} \tag{24}$$

$(\mathrm{NaNHBH_2})_\mathrm{n}$ represents a complex amorphous mixture of oligomeric and polymeric species. Temperature programmed desorption (TPD) measurements show that the second dehydrogenation step occurs in $230 - 330\,^\circ\mathrm{C}$ region. However, NaH is evident at $200\,^\circ\mathrm{C}$, which indicates the production of NaH without evolution of H_2. Specifically, Na^+ from $(\mathrm{NaNHBH_2})_\mathrm{n}$ phase can combine with hydridic hydrogen ($H^{\delta-}$) bound to boron producing sodium hydride

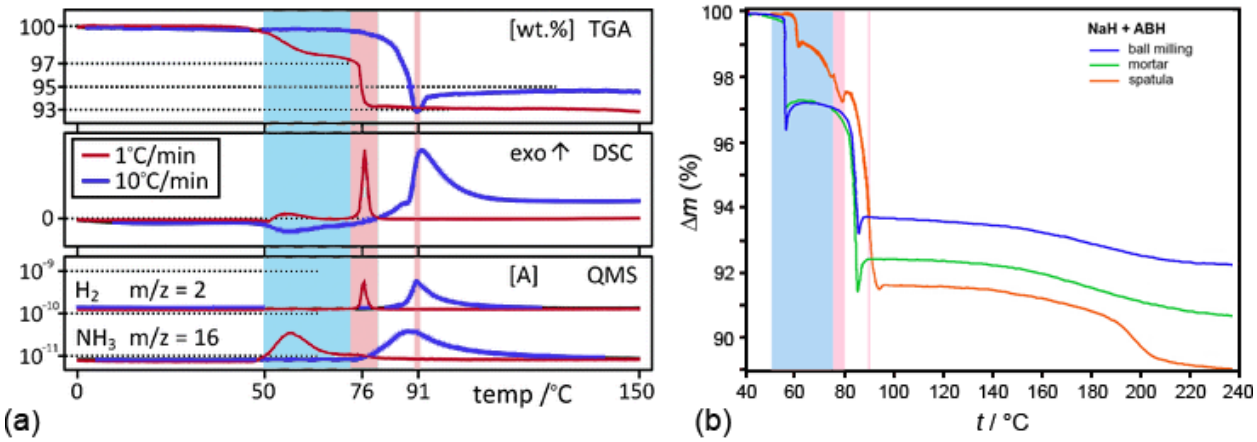

Figure 11: (a) Thermal decomposition of NaAB, as monitored by TGA, DSC and TPD. Dehydrogenation is marked with a solid grey field while the striped grey field denotes NH_3 release at heating rate $1\,^{\circ}C\,min^{-1}$. Adapted with permission from K. Fijałkowski et al. *Phys Chem. Chem. Phys.* **2012** *14* 5778. Copyright 2009 Royal Society of Chemistry. (b) TGA profiles of the products of NaH + HAB reaction as performed by different methods. Heating rate was $5\,^{\circ}C\,min^{-1}$. Adapted with permission from F.P.R. Sandra et al. *Int. J. Hydrogen En.* **2011** *36* 7423. Copyright 2011 Elsevier.

and polyimidoborane:

$$(NaNHBH_2)_n \longrightarrow nNaH + (NHBH_n \tag{25}$$

which decomposes to BN above 230 °C:

$$(NHBH_n \longrightarrow BN + nH_2(g) \tag{26}$$

It is important to note that the release of NH_3 precedes dehydrogenation of NaAB (Fig. 11, Table 4),[107] which is a serious drawback for its practical application for feeding fuel cells with H_2.[130,131] Additionally, NaAB and other alkali metal amidoboranes are not stable at room temperature and they spontaneously decompose releasing H_2 and NH_3 (Table 4).[90,93,107,124] After a few days of storing at room temperature, NaAB transforms to traces

of Na(B3N2), which is accelerated by heating NaAB to 50 °C:

$$3\,\mathrm{Na(NH_2BH_3)} \longrightarrow \mathrm{[Na(NH_3)](BH_3NH_2BH_2NH_2BH_3)} + 2\,\mathrm{[Na]} \tag{27}$$

$$\longrightarrow \mathrm{Na(BH_3NH_2BH_2NH_2BH_3)} + \mathrm{NH_3} \tag{28}$$

as described previously in the text. In reality, this process is more complex, due to the presence of unbalanced elemental sodium. Fijalkowski et al. propose a pathway to balance reaction (27) through formation of amorphous $Na_2(NH{=}BH_3)$:[124]

$$5\,\mathrm{Na(NH_2BH_3)} \longrightarrow \mathrm{[Na(NH_3)](BH_3NH_2BH_2NH_2BH_3)} + 2\,\mathrm{Na_2(NHBH_3)} + \mathrm{H_2} \tag{29}$$

However, this pathway remains only at the hypothetical level, still lacking experimental justification.

Although the isothermal TPD monitoring of dehydrogenation process during the consecutive desorption-absorption cycling is of crucial importance to deduce the applicability of materials for hydrogen storage, this characterization method was almost completely absent in the case of NaAB. Actually, measurement of isothermal dehydrogenation itself was found in only one publication (Table 4).[88] The authors have shown that NaAB evolve 6 wt % of pure H_2 during isothermal heating at 91 °C over 1 h. By holding that temperature for longer period of time (19h), almost all H_2 was released (7.4 wt % over two exothermic steps. The authors also report on unsuccesful attempt to recharge the dehydrogenated product in H_2 atmosphere at 120 bar. As mentioned before, an interesting study of NaAB decomposition employs isothermal EIS[107] in order to understand mechanistic background of the process. The characteristic maximum of the thermally-induced transition to ionic phase takes place significantly faster than in the case of other considered amidoboranes and HAB, which indicates that high sodium ion conductivity plays an important role in overall dynamics of NaAB.

On the basis of detailed DFT kinetic considerations, Kim et al. have established a

set of rules and trends explaining dehydrogenation chemistry of amidoboranes.[132] They detected that two competing mechanistic pathways take place during dehydrogenation process, namely direct and oligomeric (indirect), respectively. Conceptually, metal amidoboranes should overcome multiple-barriers to dehydrogenate. It is crucial to0 distinguish here the low- and high-temperature regime. Specifically, to dehydrogenate at lower temperatures, system should overcome a barrier determined by a minimum energy pathway, which directs the entire process. On the other hand, in high-temperature regime not only the energy barrier but also the number of steps become important determining factor. They have shown that tt 300–400 K, the dehydrogenation rate for all dimeric alkali and alkaline earth amidoboranes is pretty much the same, while NaAB show the most accelerated rates. The most important result of the study with respect to understanding of the dehydrogenation mechanism shows that the rates of oligomerization pathway and the direct pathway are comparable for lithium and sodium amidoboranes. On the other hand, potassium, calcium, and magnesium amidoboranes predominantly dehydrogenate through direct pathway. Activation energies for dehydrogenation and NH_3 release show that dehydrogenation is a preferred process, and unwanted release of NH_3 is determined by ratio of energy barriers for the two processes. Dehydrogenation rates follow the sequence LiAB > KAB > NaAB.

Decomposition of Na(B3N2) was investigated by Evans[122] and Fijalkowski.[124] NaB3N2 is very stable below 140 °C, while above this temperature it decomposes giving $NaBH_4$ through eq. (16), as justified by PXRD: ($NHBH_n$ phase is amorphous mixture of oligomeric and polymeric species. Above 200 °C ($NHBH_n$ decomposes to BN with release of H_2:

$$1/\,n(NHBH_n \longrightarrow BN + H_2 \tag{30}$$

DSC shows an endothermic event at 55 °C for NaAB,[90] (Fig. 11, Table 4) which is also observed for the product of NaH + 2 HAB.[122] These results suggest a head-to-tail thermally

activated dimerization:

$$2\,NaNH_2BH_3 \longrightarrow [NH_3Na]^+[BH_3(NHNa)BH_3]^- \tag{31}$$

analogous to well documented dimerization of HAB to DADB.[87,133] However, Fijalkowski et al. did not manage to obtain $Na(BH_3NH_2BH_3)$ in these conditions, but rather $Na(BH_3NH_2BH_2NH_2BH_3)$, through a process where $Na(BH_3NH_2BH_3)$ still may be an intermediate.[124] The alternative pathway implies a series of rearrangements leading to NaAB dimers, similar to production of DADB from HAB:[134]

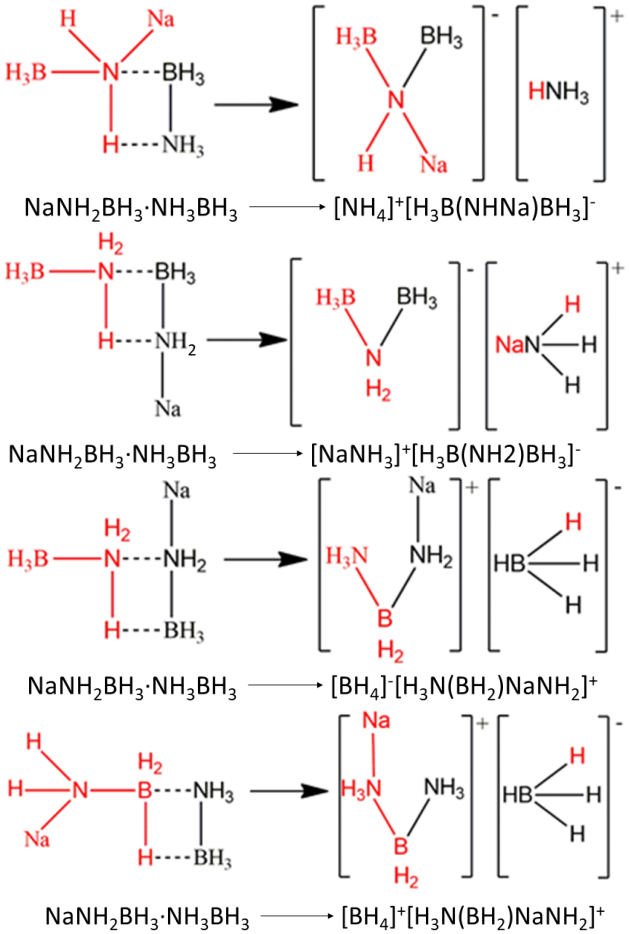

The last two reactions lead to identical products. Although all of these reactions are possible, exclusively the $[Na(NH_3)]^+[BH_2(NH_2)BH_3]^-$ leads to release of NH_3 and H_2 (Fig. 12). Thus, this process explains the endothermic event at 55 °C (Fig. 11), associated with NH_3 release. $[NH_3Na]^+[BH_3(NHNa)BH_3]^-$ can be produced also through nucleophilic attack of

$[BH_3NH_2]^-$ anion of NaAB to boron atom of HAB, which leads to $[BH_3NH_2BH_3]^-$. It combines with Na^+ giving NaADB, which is accompanied by NH_3 release. However, the observed release of NH_3 in 1 : 10 ratio with respect to H_2 leads to interpretation of NaAB decomposition as a process consisting of two different pathways, where direct decomposition of NaAB to NaNH=BH_2 dominates, while the indirect pathway through $[NH_3Na]^+[BH_3(NHNa)BH_3]^-$ represents a minor side reaction, which is responsible for NH_3 release together with a minor amount of additional H_2 (Fig. 12, Table 4).[107] In reality, the minor mechanism of the NaAB decomposition represents a superposition of all of the abovementioned reactions.

Shevlin et al. noted that the formation of a M−H−M complex as the rate-limiting step for the alkali metal amidoboranes would imply that NaAB, with the lower lattice energy for Na−H bond would dehydrogenate at a higher rate.[102] The transition state for single and dimer metal amidoborane demonstrates that the light metal atom plays a significant role in acting as a carrier for hydrogen transport during the dehydrogenation process via formation of a M−H complex. Computational results show that the presence of oligomeric intermediate structures as a rate limiting step of dehydrogenation is obvious, and the minimum dehydrogenation energy pathway from the dimeric intermediate complex involves the formation of a diammoniate of diborane. However, this requires further experimental confirmation.

Audrey et al. proposed a decomposition mechanism based at formation of polymeric B−N−H species, which results in H_2 release:[94]

$$2\,NaNH_2BH_3 \longrightarrow NaH\cdots NaNH_2BH_2NH_2BH_3 \tag{32}$$

$$\longrightarrow NaNHBH_2NaNHBH_3 + H_2 \tag{33}$$

$$\longrightarrow NaHN{=}BHNNaHBH + H_2 \tag{34}$$

Different to the above discussed decomposition processes, Ryan et al. noticed that during evolution of hydrogen ammonia is not present, which was attributed to "different synthesis methods".[103] They addressed unavoidable contamination of the reaction mixture by the

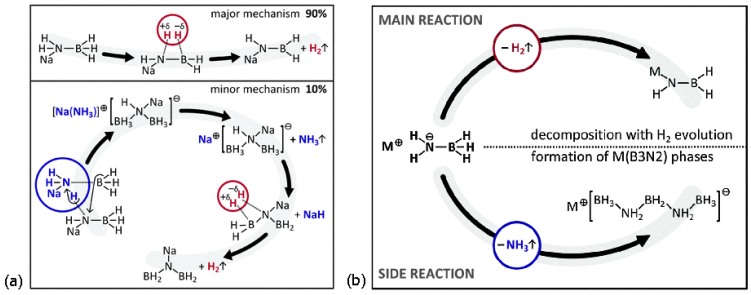

Figure 12: Thermal decomposition of alkali metal amidoboranes (exemplified by NaAB) undergoes (a) two parallel mechanistic pathways, one dominant (top) and another minor (bottom). The major pathway leads to a direct evolution of H_2, while the release of NH_3 and additional H_2 is preceded by phase transition. Reprinted with permission from K. Fijałkowski et al., *Phys. Chem. Chem. Phys.* **2012** *14* 5778. Copyright 2012 Royal Society of Chemistry. (b) Simplified expression of the process, indicating the formation of $Na(BH_3NH_2BH_2NH_2BH_3)$ through a side reaction. Reprinted with permission from K. Fijałkowski et al., *Phys. Chem. Chem. Phys.* **2014** *16* 23340. Copyright 2014 Royal Society of Chemistry.

materials from which milling jar and balls are made of during the mechanochemical process.[135–137] By this interpretation, trace quantities of impurities could act as catalysers and thus could redirect mechanochemical reaction to alternate pathways. However, the authors did not justify this hypothesis.

Whatever the low-temperature decomposition pathway was undergone by NaAB, PXRD in all cases undoubtedly show that above 250 °C the product is predominantly amorphous, while NaH remains as a dominant crystalline phase, with traces of $NaBH_4$ and BN (Table 4).[92]

Reported and perspective practical applications

As evident from the entire text and from Fig. 1, most of the references are dated from at least 5−10 years before the release of this review. Recent research interest in this field mostly abandoned amidoboranes, although some interest is still simmering.[33,59,91,139–142] However, the majority of publications in the field of amidoboranes are not focused to hydrogen storage, but to other potential applications, such as capture of CO_2 or heavy metals,[84,143,144]

Table 4: Recent developments of dehydrogenation performance of NaAB and its comparison with HAB and LiAB.

Compound	**Range** (°C)[a]	**Onset temperature** (°C)		**Released H_2** (wt.%)		Impurities	Ref.
		1st step	2nd step	1st step	2nd step		
NaAB	isothermal	70 (2040 s), 75.2 (684 s), 80.2 (94 s)	—	0.5 eq	—	n.d.	94
	isothermal	91 (1 h)	—	6.0	—		88
	isothermal	91 (19 h)	—	7.4	—	[b]	
	75 − 105	75	—	7.0	—	NH_3	90
	87 − 115	87	—	7.0	—	NH_3	107
	80 − 200	80	115	5.3	2.2	NH_3	104
	55 − 87	55	75	2.8	3.5		
	60 − 89	62	75	2.7	4.8	NH_3	92
	60 − 105	60	75	multistep, 8.3			
$\alpha - LiAB$	isothermal	80.2 (3070 s), 85.2 (698 s), 90.2 (138 s)	—	1.6	—	n.d.	94
	isothermal	91 (1 h)	—	8.0	—		88
	isothermal	91 (1 h)	—	10.9	—		
	isothermal	91 (20 h)	180 (2 h)	8.8	2.0	NH_3	109
	83 − 200	83	—	10.8	—	NH_3 (?)	118
	50 − 220	50	115	4.8	3.2	NH_3	100
	85 − 200	85	105	3.3	5.2	NH_3	64
$\beta - LiAB$	isothermal	91 (16 h)	180	8.8	2.0	NH_3	109
	85 − 200	85	105	0.9 eq	0.9 eq	n.a.	101
$LiAB \cdot HAB$	isothermal	91	180	6.0	8.3	NH_3	109
HAB	isothermal	91 (2 h)	—	4.0	< 0.1	$N_3B_3H_6$	88
	isothermal	91 (19 h)	—	5.3	—	5.3	
	100 − 200	> 100	> 120	3.2	3.3	$N_3B_3H_6$, B_2H_6, NH_3	25,28,50,138

[a] For isothermal measureents, the times are given in parentheses.
[b] The authors just declared "borazine free".

their utilization as reducing agents[145,146] and fundamental aspects of B-N compounds chemistry.[84,108,147–149]

Regarding their potential direct practical applications, the situation is even more discouraging. Namely, the utilization of the systems from this family is almost entirely limited to HAB. By the best of our knowledge, the practical applications of alkali amidoboranes are limited to reduction of α and β unsaturated aldehydes and ketones to allylic alcohols. However, among the reported reaction yields, the lowest is in the case of utilization of NaAB.[150] Additionally, potential for CO_2 capture by BN produced by pyrolysis of HAB, LiAB and NaAB was investigated.[143]

Nowadays, hypergolicity of HAB is investigated in order to produce more propulsive rocket fuels. Although the research in this regard was until now exclusively focused to HAB,[151–156] alkali amidoboranes, as more reactive derivatives, are applicable in this regard, which needs to be experimentally justified. It would be expected that NaAB, as especially reactive and relatively easily accessible system, have some potential at this point.

Conclusions and perspective

Although the family of metal amidoboranes is covered by a number of reviews, the novelty of this review is a focus to the criticism of this field with respect of potential to technological utilization of metal amidoboranes, especially NaAB as real-world systems for solid-state hydrogen storage. We have tried to argue that the richness of chemical reactivity and possible mechanistic pathways, which are very sensitive to the physical and chemical environmental conditions, make these systems impractical for any use as applicable hydrogen containers. We also proposed some new, so far unexplored or underexplored aspects of the reactivity of the NaH + HAB system.

Alkali metal hydrides readily react with HAB, which results in alkali metal amidoboranes. This is especially true for NaH, which reacts with HAB very violently. Although the

corresponding amidoboranes were reported, the reactions of HAB with KH, RbH and CsH are less studied, because of the extreme reactivity of hydrides of higher alkali metals. All alkali amidoboranes are characterized by lower dehydrogenation temperatures with respect of HAB, with still high both gravimetric and volumetric hydrogen content, which made them perspective candidate systems for solid-state hydrogen storage. Sodium amidoborane (NaAB) was recognized as a specially interesting member of this family, but a number of serious drawbacks caused the starting hype to subside with respect of technological aspects of hydrogen storage.

The outcome of volent reaction of NaH with HAB critically depends on conditions, with numerous, often hardly controllable, parameters playing a significant role. In this regard, the progression of the products $NaNH_2BH_3$ – $Na(NH_2(BH_3)_2)$ – $NaNH_2BH_3 \cdot NH_3BH_3$ – $Na(BH_3NH_2BH_2NH_2BH_3)$ is identified, which indicates numerous possible mechanistic pathways the system could take. This makes the NaH + xHAB system unique and significantly different to the analogous system including LiH.

Actually, NaH reacts with HAB upon a mere contact of these two reagents in solid state, which indicates a relatively fast solid-state diffusion in this system, while for NaAB a high Na^+ conductivity is evident. This aspect of the NaH + xHAB and related systems requires further investigations, since it potentially opens the door of its innovative applications in advanced energy systems beyond hydrogen storage.

Regarding thermal dehydrogenation of NaAB, which is the process crucial for its utilization as a source of hydrogen, it also suffers of serious technological drawbacks. Again, dehydrogenation does not lead to unique product. Rather, dehydrogenation of NaAB is branched to a complex network of mechanistic pathways, leading to even more complex mixture of linear, branched and cyclic oligomeric and polymeric species, which are thermodynamically very stable, disabling their rehydrogenation in practical conditions. Further heating finally leads to extremely stable BN.

Such a rich, complex, even chaotic chemistry makes this system practically inapplicable

for hydrogen storage in technologically practical conditions. Considering environmental aspects of its utilization, low abundance of boron makes it also highly problematic and not justified.

To conclude, alkali metal amidoboranes are not practically applicable for real-world hydrogen storage, and this is especially accentuated in the case of NaAB due to very uncontrollable dynamics of the NaH + HAB system, as reflected in its mechanochemical treatment, which shows highly vigorous and violent reactivity. However, such a vigorous reactivity of the NaH + HAB system, which can be considered as a drawback in the aspect of mechanochemistry, indicate a very fast solid-state interdiffusion of the species. Itself, such a dynamic solid-state process makes this system potentially applicable for innovative batteries, so this phenomenon requires a thorough investigation. Additionally, the NaAB (and other metal amidoboranes) was studied exclusively in the solid state, almost entirely in the context of solid-state hydrogen storage. All the other potentially interesting and technologically important physico-chemical aspects related to NaAB and other amidoboranes have not been properly addressed and investigated. In our opinion, this window is still widely opened for creative studies.

Acknowledgments

This review was written under the financial support in the framework of H2020-MSCA-IF-894705 (GrindCore) action, the Renewable Energy National Laboratory financed by the RRF-2.3.1–21- 2022–00009 project, and the Ministry of Education, Science and Technological Development of the Republic of Serbia under contract 451-03-47/2023-01/200175.

References

References

(1) Turnbull, J. C.; Graven, H.; Krakauer, N. Y. In *Radiocarbon and Climate Change: Mechanisms, Applications and Laboratory Techniques*; Schuur, E. A. G. and Druffel, E. R. M. and Trumbore, S. E., Ed.; Springer Int. Pub. AG: Cham, Switzerland, 2016; pp 83–137.

(2) Hansen, J.; Sato, M.; Kharecha, P.; von Schuckmann, K.; Beerling, D. J.; Cao, J.; Marcott, S.; Masson-Delmotte, V.; Prather, M. J.; Rohling, E. J.; Shakun, J.; Smith, P.; Lacis, A.; Russell, G.; Ruedy, R. Young people's burden: requirement of negative CO_2 emissions. *Earth Sys. Dyn.* **2017**, *8*, 577–616.

(3) Masson-Delmotte, V. et al. , Eds. *Global Warming of* 1.5 °C; IPCC, World Meteorological Organization: Geneva, Switzerland, 2018.

(4) Eyring, V.; Gillett, N.; Achuta Rao, K.; Barimalala, R.; Barreiro Parrillo, M.; Bellouin, N.; Cassou, C.; Durack, P.; Kosaka, Y.; McGregor, S.; Min, S.; Morgenstern, O.; Sun, Y. In *Climate Change 2021: The Physical Science Basis. Contribution of Working Group I to the Sixth Assessment Report of the Intergovernmental Panel on Climate Change*; Masson-Delmotte, V. et al. , Eds.; Cambridge University Press: Cambridge, United Kingdom and New York, NY, USA, 2021; p 423C552.

(5) Lee, R. The Outlook for Population Growth. *Science* **2011**, *333*, 569–573.

(6) United Nations - Department of Economic and Social Affairs; Population Division World Population Prospects 2022. https://population.un.org/wpp/Graphs/Probabilistic/POP/TOT/900.

(7) International Energy Outlook 2020. `https://www.eia.gov/outlooks/ieo/`, Accessed: 2021-03-16.

(8) Lees, N. The Brandt Line after forty years: The more North-South relations change, the more they stay the same? *Rev. Int. St.* **2021**, *47*, 85176.

(9) Kış, S.; Krajačić, G.; Duić, N.; Rosen, M. A.; Al-Nimr, M. A. Advances in integration of energy, water and environment systems towards climate neutrality for sustainable development. *En. Conv. Man.* **2020**, *225*, 113410.

(10) UNFCCC Paris Agreement. `https://unfccc.int/process-and-meetings/the-paris-agreement/the-paris-agreement`, 2015.

(11) European Commission The European Green Deal. `https://ec.europa.eu/info/strategy/priorities-2019-2024/european-green-deal/actions-being-taken-eu_en`, 2020.

(12) Balzani, V.; Bergamini, G.; Ceroni, P. Light: A Very Peculiar Reactant and Product. *Angew. Chem. Int. Ed.* **2015**, *54*, 11320–11337.

(13) Yap, K. Y.; Sarimuthu, C. R.; Lim, J. M.-Y. Virtual Inertia-Based Inverters for Mitigating Frequency Instability in Grid-Connected Renewable Energy System: A Review. *Appl. Sci.* **2019**, *9*.

(14) Hossain, E.; Faruque, H. M. R.; Sunny, M. S. H.; Mohammad, N.; Nawar, N. A Comprehensive Review on Energy Storage Systems: Types, Comparison, Current Scenario, Applications, Barriers, and Potential Solutions, Policies, and Future Prospects. *Energies* **2020**, *13*.

(15) Graetz, J.; Wolstenholme, D.; Pez, G.; Klebanoff, L.; McGrady, S.; Cooper, A. In *Hydrogen Storage Technology - Materials and Applications*; Klebanoff, L., Ed.; CRC Press, Taylor & Francis Group: Boca Raton, 2013; Chapter Development of Off-Board Reversible Hydrogen Storage Materials, pp 239–328.

(16) *Hydrogen, Fuel Cells and Infrastructure Technologies Program. Multi-Year Research, Development and Demonstration Plan. Planned Program Activities for 2005-2015*; Energy Efficiency and Renewable Energy; U.S. Department of Energy, 2011; Chapter Hydrogen Storage, 2011 Interim Update, pp 3.3–8.

(17) Bogdanović, B.; Schwickardi, M. Ti-doped alkali metal aluminium hydrides as potential novel reversible hydrogen storage materials. *J. Alloys Compds.* **1997**, *253-254*, 1–9.

(18) Anastas, P. T.; Warner, J. C. *Green Chemistry: Theory and Practice*; Oxford University Press: Oxford, UK, 2000.

(19) Dutta, S. A review on production, storage of hydrogen and its utilization as an energy resource. *J. Ind. Eng. Chem.* **2014**, *20*, 1148–1156.

(20) Villaseñor, M.; R´ ios, . Nanomaterials for water cleaning and desalination, energy production, disinfection, agriculture and green chemistry. **2018**, *16*, 11–34.

(21) Chanchetti, L. F.; Leiva, D. R.; Lopes de Faria, L. I.; Ishikawa, T. T. A scientometric review of research in hydrogen storage materials. *Int. J. Hydrogen En.* **2020**, *45*, 5356–5366.

(22) Biniwale, R. B.; Rayalu, S.; Devotta, S.; Ichikawa, M. Chemical hydrides: A solution to high capacity hydrogen storage and supply. *Int. J. Hydrogen En.* **2008**, *33*, 360–365.

(23) Orimo, S.; Nakamori, Y.; Eliseo, J. R.; Züttel, A.; Jensen, C. M. Complex Hydrides for Hydrogen Storage. *Chem. Rev.* **2007**, *107*, 4111–4132.

(24) Ley, M. B.; Jepsen, L. H.; Lee, Y.-S.; Cho, Y. W.; Bellosta von Colbe, J. M.; Dornheim, M.; Rokni, M.; Jensen, J. O.; Sloth, M.; Filinchuk, Y.; Jørgensen, J. E.; Besenbacher, F.; Jensen, T. R. Complex hydrides for hydrogen storage ? new perspectives. *Mater. Today* **2014**, *17*, 122–128.

(25) Staubitz, A.; Robertson, A. P. M.; Manners, I. Ammonia-Borane and Related Compounds as Dihydrogen Sources. *Chem. Rev.* **2010**, *110*, 4079–4124.

(26) Yu, J.; Lu, K.; Lei, W.; Hao, Q. Ammonia borane as an efficient direct fuel in alkaline fuel cells: mechanism, catalysts, applications, and challenges. *J. Mater. Chem. A* **2022**, *10*, 16779–16794.

(27) Mboyi, C. D.; Poinsot, D.; Roger, J.; Fajerwerg, K.; Kahn, M. L.; Hierso, J.-C. The Hydrogen-Storage Challenge: Nanoparticles for Metal-Catalyzed Ammonia Borane Dehydrogenation. *Small* **2021**, *17*, 2102759.

(28) Huo, J.; Zhang, K.; Wei, H.; Fu, L.; Zhao, C.; He, C.; Hu, X. A review on hydrogen production from ammonia borane: Experimental and theoretical studies. *Chin. Chem. Lett.* **2023**, *34*, 108280.

(29) Chu, H.; Qiu, S.; Sun, L.; Xu, F. In *Advanced Materials for Renewable Hydrogen Production, Storage and Utilization*; Liu, J., Ed.; IntechOpen, 2015.

(30) Owarzany, R.; Leszczyński, P. J.; Fijalkowski, K. J.; Grochala, W. Mono- and Bimetalic Amidoboranes. *Crystals* **2016**, *6*, 88.

(31) Stennett, T. E.; Harder, S. s-Block amidoboranes: syntheses, structures, reactivity and applications. *Chem. Soc. Rev.* **2016**, *45*, 1112–1128.

(32) Chua, Y. S.; Chen, P.; Wu, G.; Xiong, Z. Development of ammidoboranes for hydrogen storage. *Chem. Commun.* **2011**, *47*, 5116–5129.

(33) Castilla-Martinez, C. A.; Moury, R.; Demirci, U. B. Amidoboranes and hydrazinidoboranes: State of the art, potential for hydrogen storage, and other prospects. *Int. J. Hydrogen En.* **2020**, *45*, 30731–30755.

(34) Sato, T.; Saitoh, H.; Utsumi, R.; Ito, J.; Nakahira, Y.; Obana, K.; Takagi, S.;

Orimo, S.-i. Hydrogen Absorption Reactions of Hydrogen Storage Alloy $LaNi_5$ under High Pressure. *Molecules* **2023**, *28*.

(35) Biliškov, N.; Miletić, G. I.; Drašner, A.; Prezelj, K. Structural and hydrogen sorption properties of $SmNi_{56x}Al_x$ system C An experimental and theoretical study. *Int. J. Hydrogen En.* **2015**, *40*, 8548–8561.

(36) Barkhordarian, G.; Klassen, T.; Bormann, R. Effect of Nb_2O_5 content on hydrogen reaction kinetics of Mg. *J. Alloys Compds.* **2004**, *364*, 242–246.

(37) Barkhordarian, G.; Klassen, T.; Bormann, R. Kinetic investigation of the effect of milling time on the hydrogen sorption reaction of magnesium catalyzed with different Nb_2O_5 contents. *J. Alloys Compds.* **2006**, *407*, 249–255.

(38) Aguey-Zinsou, K.-F.; Ares Fernandez, J.; Klassen, T.; Bormann, R. Effect of Nb_2O_5 on MgH_2 properties during mechanical milling. *Int. J. Hydrogen En.* **2007**, *32*, 2400–2407.

(39) Jain, I.; Lal, C.; Jain, A. Hydrogen storage in Mg: A most promising material. *Int. J. Hydrogen En.* **2010**, *35*, 5133–5144.

(40) Ding, Z.; Li, Y.; Yang, H.; Lu, Y.; Tan, J.; Li, J.; Li, Q.; Chen, Y.; Shaw, L. L.; Pan, F. Tailoring MgH_2 for hydrogen storage through nanoengineering and catalysis. *J. Magnesium Alloys* **2022**, *10*, 2946–2967.

(41) Dragan, M. Hydrogen Storage in Complex Metal Hydrides $NaBH_4$: Hydrolysis Reaction and Experimental Strategies. *Catalysts* **2022**, *12*.

(42) Christian, M. L.; Aguey-Zinsou, K. F. CoreCShell Strategy Leading to High Reversible Hydrogen Storage Capacity for $NaBH_4$. *ACS Nano* **2012**, *6*, 7739–7751.

(43) Christian, M.; Aguey-Zinsou, K.-F. Synthesis of coreCshell $NaBH_4$@M (M = Co,

Cu, Fe, Ni, Sn) nanoparticles leading to various morphologies and hydrogen storage properties. *Chem. Commun.* **2013**, *49*, 6794–6796.

(44) Martelli, P.; Caputo, R.; Remhof, A.; Mauron, P.; Borgschulte, A.; Züttel, A. Stability and Decomposition of $NaBH_4$. *J. Phys. Chemi. C* **2010**, *114*, 7173–7177.

(45) Liu, Y.; Ren, Z.; Zhang, X.; Jian, N.; Yang, Y.; Gao, M.; Pan, H. Development of Catalyst-Enhanced Sodium Alanate as an Advanced Hydrogen-Storage Material for Mobile Applications. *En. Technol.* **2018**, *6*, 487–500.

(46) Khan, J.; Jain, I. Kinetics study of sodium alanate with catalyst TiO_2. *Renew. Sust. En. Rev.* **2015**, *52*, 504–507.

(47) Balema, V.; Pecharsky, V.; Dennis, K. Solid state phase transformations in $LiAlH_4$ during high-energy ball-milling. *J. Alloys Compds.* **2000**, *313*, 69–74.

(48) Resan, M.; Hampton, M. D.; Lomness, J. K.; Slattery, D. K. Effects of various catalysts on hydrogen release and uptake characteristics of $LiAlH_4$. *Int. J. Hydrogen En.* **2005**, *30*, 1413–1416.

(49) Resan, M.; Hampton, M. D.; Lomness, J. K.; Slattery, D. K. Effect of Ti_xAl_y catalysts on hydrogen storage properties of $LiAlH_4$ and $NaAlH_4$. *Int. J. Hydrogen En.* **2005**, *30*, 1417–1421.

(50) Wolf, G.; Baumann, J.; Baitalow, F.; Hoffmann, F. Calorimetric process monitoring of thermal decomposition of BNH compounds. *Thermochim. Acta* **2000**, *343*, 19 – 25.

(51) Stephens, F. H.; Pons, V.; Tom Baker, R. Ammonia borane: the hydrogen source par excellence? *Dalton Trans.* **2007**, 2613–2626.

(52) Demirci, U. B. Ammonia borane, a material with exceptional properties for chemical hydrogen storage. *Int. J. Hydrogen En.* **2017**, *42*, 9978–10013.

(53) Rosi, N. L.; Eckert, J.; Eddaoudi, M.; Vodak, D. T.; Kim, J.; O'Keeffe, M.; Yaghi, O. M. Hydrogen Storage in Microporous Metal-Organic Frameworks. *Science* **2003**, *300*, 1127–1129.

(54) Dillon, A. C.; Jones, K. M.; Bekkedahl, T. A.; Kiang, C. H.; Bethune, D. S.; Heben, M. J. Storage of hydrogen in single-walled carbon nanotubes. *Nature* **1997**, *386*, 377–379.

(55) Feaver, A.; Sepehri, S.; Shamberger, P.; Stowe, A.; Autrey, T.; Cao, G. Coherent Carbon Cryogel-Ammonia Borane Nanocomposites for H2 Storage. *J. Phys. Chem. B* **2007**, *111*, 7469–7472.

(56) Sepehri, S.; Garc B. B.; Cao, G. Influence of Surface Chemistry on Dehydrogenation in Carbon Cryogel Ammonia Borane Nanocomposites. *Eur. J. Inorg. Chem.* **2009**, *2009*, 599–603.

(57) Gutowska, A.; Li, L.; Shin, Y.; Wang, C. M.; Li, X. S.; Linehan, J. C.; Smith, R. S.; Kay, B. D.; Schmid, B.; Shaw, W.; Gutowski, M.; Autrey, T. Nanoscaffold Mediates Hydrogen Release and the Reactivity of Ammonia Borane. *Angew. Chem. Int. Ed. Engl.* **2005**, *44*, 3578–3582.

(58) Yang, J.; Sudik, A.; Wolverton, C.; Siegel, D. J. High capacity hydrogen storage materials: attributes for automotive applications and techniques for materials discovery. *Chem. Soc. Rev.* **2010**, *39*, 656–675.

(59) Milanović, I.; Biliškov, N.; Užarević, K.; Lukin, S.; Etter, M.; Halasz, I. Mechanochemical Synthesis and Thermal Dehydrogenation of Novel Calcium-Containing Bimetallic Amidoboranes. *ACS Sust. Chem. Eng.* **2021**, *9*, 2089–2099.

(60) Biliškov, N. Infrared spectroscopic monitoring of solid-state processes. *Phys. Chem. Chem. Phys.* **2022**, *24*, 19073–19120.

(61) Luo, J.; Kang, X.; Wang, P. Synthesis, formation mechanism, and dehydrogenation properties of the long-sought $Mg(NH_2BH_3)_2$ compound. *En. Environ. Sci.* **2013**, *6*, 1018–1025.

(62) Kondrat'ev, Y. V.; Butlak, A.; Kazakov, I.; Krasnova, I.; Chislov, M.; Timoshkin, A. Y. Heat Effects of the Thermal Decomposition of Amidoboranes of Potassium, Calcium, and Strontium. *Russ. J. Phys. Chem. A* **2018**, *92*, 640 – 645.

(63) Kobayashi, T.; Hlova, I. Z.; Singh, N. K.; Pecharsky, V. K.; Pruski, M. Solid-state NMR study of Li-assisted dehydrogenation of ammonia borane. *Inorg. Chem.* **2012**, *51*, 4108 – 4115.

(64) Shimoda, K.; Doi, K.; Nakagawa, T.; Zhang, Y.; Miyaoka, H.; Ichikawa, T.; Tansho, M.; Shimizu, T.; Burrell, A. K.; Kojima, Y. Comparative study of structural changes in NH_3BH_3, $LiNH_2BH_3$, and KNH_2BH_3 during dehydrogenation process. *J. Phys. Chem. C* **2012**, *116*, 5957 – 5964.

(65) Roy, B.; Pal, U.; Bishnoi, A.; O'Dell, L. A.; Sharma, P. Exploring the homopolar dehydrocoupling of ammonia borane by solid-state multinuclear NMR spectroscopy. *Chem. Commun.* **2021**, *57*, 1887–1890.

(66) Comanescu, C. Paving the Way to the Fuel of the Futuremdash;Nanostructured Complex Hydrides. *Int. J. Mol. Sci.* **2023**, *24*, 143.

(67) Petit, J. F.; Demirci, U. B. Discrepancy in the thermal decomposition/dehydrogenation of ammonia borane screened bythermogravimetric analysis. *Int. J. Hydrogen En.* **2019**, *44*, 14201–14206.

(68) Zhu, H.; Cheng, H.; Chen, D.; Ding, Z. Development of compact and efficient volumetric apparatus for measuring absorption/desorption properties of hydrogen storage materials. *Int. J. Hydrogen En.* **2022**, *47*, 32565–32581.

(69) Broom, D. The accuracy of hydrogen sorption measurements on potential storage materials. *Int. J. Hydrogen En.* **2007**, *32*, 4871 – 4888.

(70) Kamruddin, M.; Ajikumar, P.; Dash, S.; Tyagi, A.; Raj, B. Thermogravimetry-evolved gas analysis-mass spectrometry system for materials research. *Bull. Mater. Sci.* **2003**, *26*, 449 – 460.

(71) Gac, W.; Zawadzki, W.; Rotko, M.; Greluk, M.; Slowik, G.; Kolb, G. Effects of support composition on the performance of nickel catalysts in CO_2 methanation reaction. *Catalysis Today* **2020**, *357*, 468 – 482.

(72) Ingman, E. R.; Shepherd, A.; Brown, W. A. Using surface science techniques to investigate the interaction of acetonitrile with dust grain analogue surfaces behaviour of acetonitrile and water on a graphitic surface. *Johnson Matthey Technol. Rev.* **2021**, *65*, 600 – 614.

(73) Shore, S. G.; Parry, R. W. The crystalline compound ammonia-borane, H_3NBH_3. *J. Am. Chem. Soc.* **1955**, *77*, 6084–6085.

(74) Heldebrant, D. J.; Karkamkar, A.; Linehan, J. C.; Autrey, T. Synthesis of ammonia borane for hydrogenstorage applications. *En. Environ. Sci.* **2008**, *1*, 156–160.

(75) Filinchuk, Y.; Nevidomskyy, A. H.; Chernyshov, D.; Dmitriev, V. High-pressure phase and transition phenomena in ammonia borane NH_3BH_3 from X-ray diffraction, Landau theory, and ab initio calculations. *Phys. Rev. B* **2009**, *79*, 214111.

(76) Al-Kukhun, A.; Hwang, H. T.; Varma, A. Mechanistic studies of ammonia borane dehydrogenation. *Int. J. Hydrogen En.* **2013**, *38*, 169–179.

(77) Biliškov, N.; Borgschulte, A.; Užarević, K.; Halasz, I.; Lukin, S.; Milošević, S.; Milanović, I.; Grbović Novaković, J. In-Situ and Real-time Monitoring of Mechanochem-

ical Preparation of $Li_2Mg(NH_2BH_3)_4$ and $Na_2Mg(NH_2BH_3)_4$ and Their Thermal Dehydrogenation. *Chem. Eur. J.* **2017**, *23*, 16274–16282.

(78) Geanangel, R.; Wendlandt, W. A TGDSC study of the thermal dissociation of (NH2BH2)x. *Thermochim. Acta* **1985**, *86*.

(79) Bowden, M.; Autrey, T.; Brown, I.; Ryan, M. The thermal decomposition of ammonia borane: A potential hydrogen storage material. *Curr. Appl. Phys.* **2008**, *8*, 498–500.

(80) Baitalow, F.; Baumann, J.; Wolf, G.; Jaenicke-Rössler; Leitner, G. Thermal decomposition of B-N-H compounds investigated by using combined thermoanalytical methods. *Thermochim. Acta* **2002**, *391*, 159–168.

(81) Kisu, K.; Kim, S.; Inukai, M.; Oguchi, H.; Takagi, S.; Orimo, S.-i. Magnesium Borohydride Ammonia Borane as a Magnesium Ionic Conductor. *ACS Appl. En. Mater.* **2020**, *3*, 3174–3179.

(82) Palumbo, M.; Kisu, K.; Gulino, V.; Nervi, C.; Maschio, L.; Casassa, S.; Orimo, S.-i.; Baricco, M. Ion Conductivity in a Magnesium Borohydride Ammonia Borane Solid-State Electrolyte. *J. Phys. Chem. C* **2022**, *126*, 15118–15127.

(83) Chernysheva, A.; Shelyganov, P.; Kazakov, I.; Timoshkin, A. Complex amidoboranes $M''[M'(NH_2BH_3)_4]$ (M' = Al, Ga; M" = Li, Na, K, Rb, Cs). *Russ. J. Gen. Chem.* **2017**, *87*, 665–669.

(84) Kirkina, V. A.; Kissel, A. A.; Selikhov, A. N.; Nelyubina, Y. V.; Filippov, O. A.; Belkova, N. V.; Trifonov, A. A.; Shubina, E. S. Amine-boranes reactions promoted by lanthanide(ii) ions. *Chem. Commun.* **2022**, *58*, 859–862.

(85) Callini, E. et al. Nanostructured materials for solid-state hydrogen storage: A review of the achievement of COST Action MP1103. *Int. J. Hydrogen En.* **2016**, *41*, 14404–14428.

(86) Dovgaliuk, I.; Filinchuk, Y. Aluminium complexes of B- and N-based hydrides: Synthesis, structures and hydrogen storage properties. *Int. J. Hydrogen En.* **2016**, *41*, 15489–15504.

(87) Schlesinger, H. I.; Burg, A. B. Hydrides of Boron. VIII. The Structure of the Diammoniate of Diborane and its Relation to the Structure of Diborane. *J. Am. Chem. Soc.* **1938**, *60*, 290–299.

(88) Xiong, Z.; Yong, C. K.; Wu, G.; Chen, P.; Shaw, W.; Karkamkar, A.; Autrey, T.; Jones, M. O.; Johnson, S. R.; Edwards, P. P.; David, W. I. F. High-capacity hydrogen storage in lithium and sodium amidoboranes. *Nature Mater.* **2008**, *7*, 138–141.

(89) Xiong, Z.; Wu, G.; Chua, Y. S.; Hu, J.; He, T.; Xu, W.; Chen, P. Synthesis of sodium amidoborane ($NaNH_2BH_3$) for hydrogen production. *Energy Environ. Sci.* **2008**, *1*, 360–363.

(90) Fijalkowski, K. J.; Grochala, W. Substantial emission of NH_3 during thermal decomposition of sodium amidoborane, $NaNH_2BH_3$. *J. Mater. Chem.* **2009**, *19*, 2043–2050.

(91) Milanović, I.; Biliškov, N. Mechanochemical pretreatment of ammonia borane: A new procedure for sodium amidoborane synthesis. *Int. J. Hydrogen En.* **2020**, *45*, 7938–7946.

(92) Sandra, F.; Demirci, U.; Chiriac, R.; Moury, R.; Miele, P. A simple preparation method of sodium amidoborane, highly efficient derivative of ammonia borane dehydrogenating at low temperature. *Int. J. Hydrogen En.* **2011**, *36*, 7423–7430.

(93) Fijalkowski, K. J.; Genova, R. V.; Filinchuk, Y.; Budzianowski, A.; Derzsi, M.; Jaron, T.; Leszczynski, P. J.; Grochala, W. $Na[Li(NH_2BH_3)_2]$ – the first mixed-cation amidoborane with unusual crystal structure. *Dalton Trans.* **2011**, *40*, 4407–4413.

(94) Luedtke, A. T.; Autrey, T. Hydrogen Release Studies of Alkali Metal Amidoboranes. *Inorg. Chem.* **2010**, *49*, 3905–3910.

(95) Lee, T. B.; McKee, M. L. Mechanistic Study of $LiNH_2BH_3$ Formation from $(LiH)_4$ + NH_3BH_3 and Subsequent Dehydrogenation. *Inorg. Chem.* **2009**, *48*, 7564–7575.

(96) Miranda, C. R.; Ceder, G. Ab initio investigation of ammonia-borane complexes for hydrogen storage. *J. Chem. Phys.* **2007**, *126*, 184703.

(97) Hughes, E. W. The Crystal Structure of Ammonia-borane, H_3NBH_3. *J. Am. Chem. Soc.* **1956**, *78*, 502–503.

(98) Reynhardt, E. C.; Hoon, C. F. Molecular dynamics and structures of amine boranes of the type $R_3N \cdot BH_3$. II. NMR investigation of $H_3N \cdot BH_3$. *J. Phys. C: Solid St. Phys.* **1983**, *16*, 6137–6152.

(99) Klooster, W. T.; Koetzle, T. F.; Siegbahn, P. E. M.; Richardson, T. B.; Crabtree, R. H. Study of the N−H···H−B Dihydrogen Bond Including the Crystal Structure of BH_3NH_3 by Neutron Diffraction. *J. Am. Chem. Soc.* **1999**, *121*, 6337–6343.

(100) Diyabalanage, H. V. K.; Nakagawa, T.; Shrestha, R. P.; Semelsberger, T. A.; Davis, B. L.; Scott, B. L.; Burrell, A. K.; David, W. I. F.; Ryan, K. R.; Jones, M. O.; Edwards, P. P. Potassium(I) Amidotrihydroborate: Structure and Hydrogen Release. *J. Am. Chem. Soc.* **2010**, *132*, 11836–11837.

(101) Wu, H.; Zhou, W.; Yildirim, T. Alkali and Alkaline-Earth Metal Amidoboranes: Structure, Crystal Chemistry, and Hydrogen Storage Properties. *J. Am. Chem. Soc.* **2008**, *130*, 14834–14839.

(102) Shevlin, S. A.; Kerkeni, B.; Guo, Z. X. Dehydrogenation mechanisms and thermodynamics of MNH_2BH_3 (M = Li, Na) metal amidoboranes as predicted from first principles. *Phys. Chem. Chem. Phys.* **2011**, *13*, 7649–7659.

(103) Ryan, K. R. A study of ammonia borane and its derivatives. Ph.D. thesis, Oxford University, UK, 2011.

(104) Shimoda, K.; Yamane, A.; Ichikawa, T.; Kojima, Y. First-Principles Calculations of Potassium Amidoborane KNH_2BH_3: Structure and ^{39}K NMR Spectroscopy. *J. Phys. Chem. C* **2012**, *116*, 20666–20672.

(105) Owarzany, R.; Jaroń, T.; Leszczyński, P. J.; Fijałkowski, K. J.; Grochala, W. Amidoboranes of rubidium and caesium: the last missing members of the alkali metal amidoborane family. *Dalton Trans.* **2017**, *46*, 16315–16320.

(106) Wolstenholme, D. J.; Titah, J. T.; Che, F. N.; Traboulsee, K. T.; Flogeras, J.; McGrady, G. S. Homopolar Dihydrogen Bonding in Alkali-Metal Amidoboranes and Its Implications for Hydrogen Storage. *J. Am. Chem. Soc.* **2011**, *133*, 16598–16604.

(107) Fijalkowski, K. J.; Jurczakowski, R.; Kozminski, W.; Grochala, W. Insights from impedance spectroscopy into the mechanism of thermal decomposition of $M(NH_2BH_3)$, M = H, Li, Na, $Li_{0.5}Na_{0.5}$, hydrogen stores. *Phys. Chem. Chem. Phys.* **2012**, *14*, 5778–5784.

(108) Magos-Palasyuk, E.; Litwiniuk, A.; Palasyuk, T. Experimental and theoretical evidence of dihydrogen bonds in lithium amidoborane. *Sci. Rep.* **2020**, *10*, 17431.

(109) Wu, C.; Wu, G.; Xiong, Z.; David, W. I. F.; Ryan, K. R.; Jones, M. O.; Edwards, P. P.; Chu, H.; Chen, P. Stepwise Phase Transition in the Formation of Lithium Amidoborane. *Inorg. Chem.* **2010**, *49*, 4319–4323.

(110) Ramzan, M.; Silvearv, F.; Blomqvist, A.; Scheicher, R. H.; Lebègue, S.; Ahuja, R. Structural and energetic analysis of the hydrogen storage materials $LiNH_2BH_3$ and $NaNH_2BH_3$ from ab initio calculations. *Phys. Rev. B* **2009**, *79*, 132102.

(111) Magos-Palasyuk, E.; Fijalkowski, K. J.; Palasyuk, T. Chemically driven negative linear compressibility in sodium amidoborane, $Na(NH_2BH_3)$. *Sci. Rep.* **2016**, *6*, 28745.

(112) Chen, X.-M.; Li, H.; Yang, Q.-Y.; Wang, R.-R.; Hamilton, E. J. M.; Zhang, J.; Chen, X. Brnsted and Lewis Base Behavior of Sodium Amidotrihydridoborate ($NaNH_2BH_3$). *Eur. J. Inorg. Chem.* **2017**, *2017*, 4541–4545.

(113) DeGraffenried, A. L. Studies on Boron - Nitrogen and Boron - Gadolinium Compounds. Ph.D. thesis, The Ohio State University, 1995.

(114) Daly, S. R.; Bellott, B. J.; Kim, D. Y.; Girolami, G. S. Synthesis of the Long-Sought Unsubstituted Aminodiboranate $Na(H_3B{-}NH_2{-}BH_3)$ and Its N-Alkyl Analogs. *J. Am. Chem. Soc.* **2010**, *132*, 7254–7255.

(115) Chen, W.; Yu, H.; Wu, G.; He, T.; Li, Z.; Guo, Z.; Liu, H.; Huang, Z.; Chen, P. Ammonium Aminodiboranate: A Long-Sought Isomer of Diammoniate of Diborane and Ammonia Borane Dimer. *Chem. Eur. J.* **2016**, *22*, 7727–7729.

(116) Burrell, A. K. Metal Aminoboranes; US Patent No. 7713506. 2010.

(117) Shore, S. G.; Parry, R. W. Chemical Evidence for the Structure of the Diammoniate of Diborane. II. The Preparation of Ammonia-Borane. *J. Am. Chem. Soc.* **1958**, *80*, 8–12.

(118) Kang, X.; Fang, Z.; Kong, L.; Cheng, H.; Yao, X.; Lu, G.; Wang, P. Ammonia Borane Destabilized by Lithium Hydride: An Advanced On-Board Hydrogen Storage Material. *Adv. Mater.* **2008**, *20*, 2756–2759.

(119) Diyabalanage, H. V. K.; Shrestha, R. P.; Semelsberger, T. A.; Scott, B. L.; Bowden, M. E.; Davis, B. L.; Burrell, A. K. Calcium Amidotrihydroborate: A Hydrogen Storage Material. *Angew. Chem. Int. Ed.* **2007**, *46*, 8995–8997.

(120) Ardila-Fierro, K. J.; Hernández, J. G. Sustainability Assessment of Mechanochemistry by Using the Twelve Principles of Green Chemistry. *ChemSusChem* **2021**, *14*, 2145–2162.

(121) Chen, W.; Huang, Z.; Wu, G.; Chen, P. New synthetic procedure for $NaNH_2(BH_3)_2$ and evaluation of its hydrogen storage properties. *Sci. Chin. Chem.* **2015**, *58*, 169–173.

(122) Evans, I. C. Metallated derivatives of ammonia borane with a view to their potential as hydrogen storage materials. Ph.D. thesis, University of Birmingham, 2011.

(123) Li, H.; Ma, N.; Meng, W.; Gallucci, J.; Qiu, Y.; Li, S.; Zhao, Q.; Zhang, J.; Zhao, J.-C.; Chen, X. Formation Mechanisms, Structure, Solution Behavior, and Reactivity of Aminodiborane. *J. Am. Chem. Soc.* **2015**, *137*, 12406–12414.

(124) Fijalkowski, K. J.; Jaron, T.; Leszczynski, P. J.; Magos-Palasyuk, E.; Palasyuk, T.; Cyranski, M. K.; Grochala, W. $M(BH_3NH_2BH_2NH_2BH_3)$ - the missing link in the mechanism of the thermal decomposition of light alkali metal amidoboranes. *Phys. Chem. Chem. Phys.* **2014**, *16*, 23340–23346.

(125) Owarzany, R.; Fijalkowski, K. J.; Jaroń, T.; Leszczyński, P. J.; Dobrzycki, L.; Cyrański, M. K.; Grochala, W. Complete Series of Alkali-Metal $M(BH_3NH_2BH_2NH_2BH_3)$ Hydrogen-Storage Salts Accessed via Metathesis in Organic Solvents. *Inorg. Chem.* **2016**, *55*, 37–45.

(126) Zhang, Y.; Wolverton, C. *J. Phys. Chem. C* **2012**, *116*, 14224–14231.

(127) Zhang, Y.; Autrey, T.; Wolverton, C. *J. Phys. Chem. C* **2012**, *116*, 26728–26734.

(128) Qi, S.; Yan, J.; Shi, L.; Tan, X. Direct pyrolysis dehydrogenation mechanism of ammonia borane and alkali metal substituted ammonia borane. *Chem. Eng. Trans.* **2020**, *81*, 1309–1314.

(129) Pomogaeva, A. V.; Morokuma, K.; Timoshkin, A. Y. Trimeric cluster of lithium amidoborane - the smallest unit for the modeling of hydrogen release mechanism. *J. Comput. Chem.* **2016**, *37*, 1259–1264.

(130) Rajalakshmi, N.; Jayanth, T.; Dhathathreyan, K. Effect of Carbon Dioxide and Ammonia on Polymer Electrolyte Membrane Fuel Cell Stack Performance. *Fuel Cells* **2003**, *3*, 177–180.

(131) Halseid, R.; Vie, P. J.; Tunold, R. Effect of ammonia on the performance of polymer electrolyte membrane fuel cells. *J. Power Sources* **2006**, *154*, 343–350.

(132) Kim, D. Y.; Lee, H. M.; Seo, J.; Shin, S. K.; Kim, K. S. Rules and trends of metal cation driven hydride-transfer mechanisms in metal amidoboranes. *Phys. Chem. Chem. Phys.* **2010**, *12*, 5446–5453.

(133) Stowe, A. C.; Shaw, W. J.; Linehan, J. C.; Schmid, B.; Autrey, T. In situ solid state 11B MAS-NMR studies of the thermal decomposition of ammonia borane: mechanistic studies of the hydrogen release pathways from a solid state hydrogen storage material. *Phys. Chem. Chem. Phys.* **2007**, *9*, 1831–1836.

(134) Mayer, E. Symmetrical cleavage of diborane by ammonia in solution. *Inorg. Chem.* **1972**, *11*, 866–869.

(135) Kim, S. Y.; Choi, D. K.; Yeo, D.-H.; Shin, H. S.; Yoon, H. G. Influence of ball milling contamination on properties of sintered AlN substrates. *J. Eur. Ceramic Soc.* **2020**, *40*, 5349–5356.

(136) Štefanić, G.; Krehula, S.; Štefanić, I. Phase development during high-energy ball-milling of zinc oxide and iron C the impact of grain size on the source and the degree of contamination. *Dalton Trans.* **2015**, *44*, 18870–18881.

(137) Di Nardo, T.; Moores, A. Mechanochemical amorphization of chitin: Impact of apparatus material on performance and contamination. *Beilstein J. Org. Chem.* **2019**, *15*, 1217–1225.

(138) Hu, M.; Geanangel, R.; Wendlandt, W. *Thermochim. Acta* **1978**, *23*, 249–255.

(139) Zhong, J.; Dai, W.; Leng, H.; Li, Q. Improvement of dehydrogenation performance of $NH_3BH_3-KNH_2BH_3$ composites. *J. Alloys Compds.* **2022**, *928*, 167113.

(140) Liu, X.; Wang, S.; Wu, Y.; Li, Z.; Jiang, L.; Guo, X.; Ye, J. Dehydrogenation properties of two phases of $LiNH_2BH_3$. *Int. J. Hydrogen En.* **2020**, *45*, 2127 – 2134.

(141) Liu, X.; Wu, Y.; Wang, S.; Li, Z.; Guo, X.; Ye, J.; Jiang, L. Current progress and research trends on lithium amidoborane for hydrogen storage. *J. Mater. Sci.* **2020**, *55*, 2645 – 2660.

(142) Lv, N.-x.; Tao, J.-c.; Li, H.-p. The theoretical study of dehydrogenation mechanism from Sr(NH2BH3)2. *Struct. Chem.* **2020**, *31*, 339 ? 350.

(143) Castilla-Martinez, C. A.; Mighri, R.; Charmette, C.; Cartier, J.; Demirci, U. B. Boron Nitride from Ammonia Borane and Alkali Amidoboranes and Its Features for Carbon Dioxide Capture. *Energy Technol.* **2023**, *11*, 2201521.

(144) Kiernicki, J. J.; Zeller, M.; Szymczak, N. K. Examining the Generality of Metal-Ligand Cooperativity across a Series of First-Row Transition Metals: Capture, Bond Activation, and Stabilization. *Inorg. Chem.* **2020**, *59*, 9279 – 9286.

(145) Guo, Y.; Wang, R.-Y.; Kang, J.-X.; Ma, Y.-N.; Xu, C.-Q.; Li, J.; Chen, X. Efficient synthesis of primary and secondary amides via reacting esters with alkali metal amidoboranes. *Nature Commun.* **2021**, *12*, 5964.

(146) Peng, J.; Song, Y.; Wang, Y.; Liu, Z.; Chen, X. Catalyst-free reductions of nitriles

to amino-boranes using sodium amidoborane and lithium borohydride. *Org. Chem. Front.* **2022**, *9*, 1536 – 1540.

(147) Ju, M.-Y.; Guo, Y.; Chen, X.-M.; Chen, X. Facile Synthetic Method of $Na[BH_3(NH_2BH_2)_2H]$ Based on the Reactions of Sodium Amidoborane ($NaNH_2BH_3$) with $NiBr_2$ or $CoCl_2$. *Inorg. Chem.* **2021**, *60*, 7101 – 7107.

(148) Nawrocka, E. K.; Prus, A.; Owarzany, R.; Koźmiński, W.; Kazimierczuk, K.; Fijalkowski, K. J. The assignment of ^{11}B and ^{1}H resonances in the post-reaction mixture from the dry synthesis of $Li(BH_3NH_2BH_2NH_2BH_3)$. *Magn. Reson. Chem.* **2023**, *61*, 49 – 54.

(149) Zhang, T.; Steenhaut, T.; Li, X.; Devred, F.; Devillers, M.; Filinchuk, Y. Aluminum methylamidoborane complexes: mechanochemical synthesis, structure, stability, and reactive hydride composites. *Sust. En. Fuels* **2023**, *7*, 1119 – 1126.

(150) Weiliang, X. Application of Ammonia Borane and Metal Amidoboranes in Organic Reduction. Ph.D. thesis, NATIONAL UNIVERSITY OF SINGAPORE, 2012.

(151) Baier, M. J.; Ramachandran, P. V.; Son, S. F. Characterization of the hypergolic ignition delay of ammonia borane. *J. Propul. Power* **2019**, *35*, 182 – 189.

(152) Baier, M. J.; McDonald, A. J.; Clements, K. A.; Goldenstein, C. S.; Son, S. F. High-speed multi-spectral imaging of the hypergolic ignition of ammonia borane. *Proc. Combust. Inst.* **2021**, *38*, 4433 – 4440.

(153) Baier, M. J.; Jarocki, C. M.; Noel, A. R.; Son, S. F. Performance enhancement and ignition delay suppression of TMEDA using amine-borane additives. *Int. J. En. Mater. Chem. Propul.* **2022**, *21*, 77 – 91.

(154) Jeong, J.; Kim, K. S.; Bhosale, V. K.; Kwon, S. Demonstration of ammonia borane-based hypergolic ignitor for hybrid rocket. *Acta Astronaut.* **2022**, *196*, 85–93.

(155) Clements, K. A.; Baier, M. J.; Veeraraghavan Ramachandran, P.; Son, S. F. Experimental study of factors affecting hypergolic ignition of ammonia borane. *J. Propul. Power* **2021**, *37*, 202 – 210.

(156) Seo, J. E.; Kim, Y.; Kim, Y.; Kim, K.; Lee, J. H.; Lee, D. H.; Kim, Y.; Shin, S. J.; Kim, D. M.; Kim, S. Y.; Kim, T.; Yoon, C. W.; Nam, S. W. Portable ammonia-borane-based H_2 power-pack for unmanned aerial vehicles. *J. Power Sources* **2014**, *254*, 329 – 337.